2023

Identification of New Substrates from Pseudomonas Aeruginosa Exos

Adam V. Thota

LOYOLA UNIVERSITY CHICAGO

IDENTIFICATION OF NEW SUBSTRATES FROM *PSEUDOMONAS AERUGINOSA* EXOS

A THESIS SUBMITTED TO

THE FACULTY OF THE GRADUATE SCHOOL

IN CANDIDACY FOR THE DEGREE OF

MASTER OF SCIENCE

PROGRAM IN BIOCHEMISTRY AND MOLECULAR BIOLOGY

BY

ADAM V THOTA

CHICAGO, ILLINOIS

AUGUST 2023

ACKNOWLEDGEMENTS

I would like to thank Dr Abby Kroken, PhD, for welcoming me into the lab and helping me become the scientist I can be. Before joining the lab, I was uncertain about my career, but I am now excited to continue improving as a scientist. Moreover, I would like to thank my current and former lab members, especially Rachel Mazurek. You have been a great friend and someone I can bounce ideas off of.

I would like to thank the other members of my thesis committee: Dr Jonathan Kirk and Dr Jonathan Allen for their ideas and guidance throughout my thesis. They have both been great mentors and collaborators, while helping me with skills that I will continue to use in my studies.

Lastly, I would like to thank my friends and family for supporting me through my education. I would not be the man I am today without their love and support over the years.

TABLE OF CONTENT

LIST OF TABLES

LIST OF FIGURES

CHAPTER ONE

BACKGROUND

Review of Literature

Overview

Pseudomonas aeruginosa is a gram-negative environmental bacterium that uses its intrinsic and acquired antibiotic resistance to infect patients with compromised epithelium, such as in cystic fibrosis and burn wounds. It is also a common hospital acquired infection (1). *P. aeruginosa* is also one of the leading causes of corneal infections, termed keratitis. (2, 3). The healthy ocular surface normally provides robust antimicrobial protection against pathogens. Corneal infection is often the result of either injury (introducing bacteria directly into the corneal stroma), or improper contact lens hygiene practices, both of which compromise epithelial health and barrier function (4). In order to cause disease, most strains of *P. aeruginosa* typically use a virulence factor, the type three secretion system (T3SS), to disrupt cellular signaling or for cytotoxicity (5). In addition, if the corneal epithelium is compromised, *P. aeruginosa* can become intracellular to establish cytosolic niches. During cellular invasion, the expression of the T3SS is first required for *P. aeruginosa* to escape from membrane bound vacuoles (Fig 1A) (6). *P. aeruginosa* then secretes exotoxins, from inside vacuoles or once cytosolic, to prolong host cell death (6). This delay of host cell lysis seems to be necessary for *P. aeruginosa* to establish intracellular niches. Of the T3 secreted effector toxins, ExoS, specifically the ADP-ribosyltransferase activity of ExoS, was shown to prolong the death of invaded corneal cells (7).

Moreover, ExoS becomes dispensable for maintaining intact intracellular niches when caspase-4 is knocked out, suggesting ExoS interferes with the completion of caspase-4 mediated pyroptosis (8). While ExoS has no known substrates involved in caspase-4 mediated cell death, other groups have demonstrated that many potential ExoS substrates remain uncategorized (9, 10).

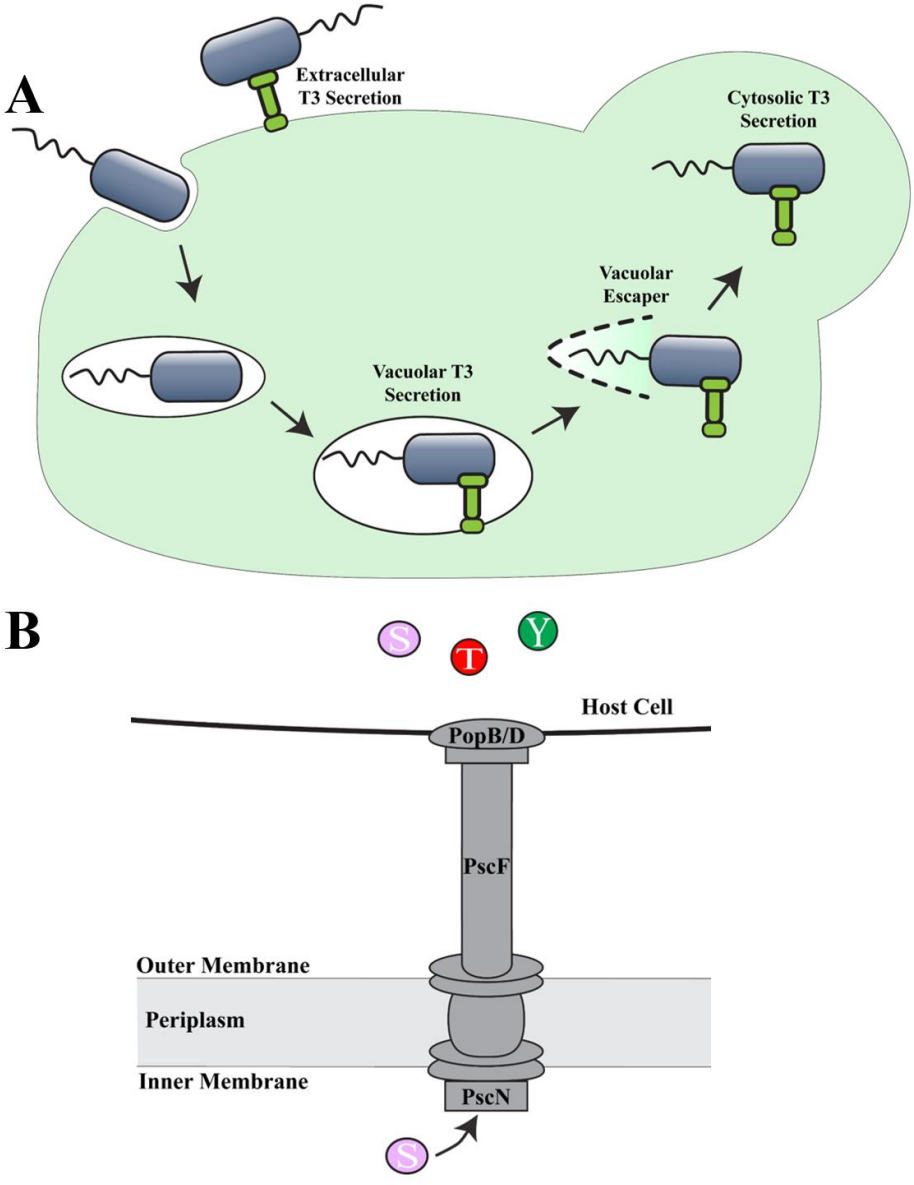

Figure 1. ***P. aeruginosa*** **Lifestyle and T3SS. (A)** Diagram of the *P. aeruginosa* intracellular and extracellular lifestyle. **(B)** Diagram of the type three secretion system (T3SS). Adapted from Galle M, et al. Curr Protein Pept Sci. 2012 Dec;13(8):831-42.

Introduction to the Type Three Secretion System and Exotoxins

P. aeruginosa utilizes its Type Three Secretion System (T3SS) for both acute virulence and, more recently shown, to accomplish intracellular replication within several types of epithelial cells (7). The T3SS is a needle-like structure spanning the inner and outer membranes of bacteria, extracellular space, and to the host plasma membrane (Fig.1 B) (11). Critical components of the T3SS include PscF, the needle; PopB/D, the needle tip; and PscN, an ATPase that pushes the exotoxins through the needle (Fig 1B) (12).

Using the T3SS, *P. aeruginosa* secretes four known effector toxins: ExoS, ExoT, ExoY, and ExoU. ExoU is a phospholipase that can lyse the host cell membrane and is only found in cytotoxic *P. aeruginosa* strains, which do not exhibit an intracellular lifestyle due to rapidly killing target host cells (13-15). ExoY is a nucleotidyl cyclase that contributes to both the rounding of host cells as well as reducing cytotoxicity in some contexts (16-18). ExoS and ExoT are bifunctional enzymes with an N-terminal Rho GTPase Activating Protein (Rho GAP) domain and a C-terminal mono ADP-ribosyl transferase (ADPr) domain (19-23). The Rho GAP domain of both toxins targets the proteins Rho, Rac, and Cdc42 resulting in the disruption of the actin cytoskeleton (24). ExoT mono ADP-ribosylates Crk1 and Crk2, which disrupts focal adhesion assembly during infection (25, 26). The ADPr domain of ExoS has a broader range of substrates including small GTPases (Ras, Rap1, Rab proteins: 5 ,7, 8, and 11) to disturb intracellular trafficking (Table 1) (27-32). ExoS also targets Ezrin, Radixin, and Moesin (ERM proteins) which impacts cytoskeletal connections to plasma membrane (33, 34). Other ExoS substrates include vimentin, cyclophilin A, and Cdc42 (10, 24, 35).

Table 1. Known ExoS ADP-ribosylation Substrates.

Substrate	Weight kDa	Site	Reference
Cyclophilin A	18	R55, R69	DiNovo et al, 2006
Rap1b	21	R41	Riese et al, 2001
N-Ras	21	R41	Vincent et al, 1999
Cdc42	21		Goehring et al, 1999
H-Ras	21	R41	Vincent et al, 1999
Rac1	21		Rocha et al, 2005
K-Ras	21	R41	Vincent et al, 1999
Rab7	23		Fraylick et al, 2002
RalA	23		Fraylick et al, 2002
Rab5	23	R81,91,110,120,195,197	Barbieri of al, 2001
Rab8	24		Fraylick et al, 2002
Rab11	24		Rocha et al, 2005
Vimentin	53		Coburn et al, 1989
Moesin	68		Maresso et al, 2004
Radixin	68		Maresso et al, 2004
Ezrin	69		Maresso et al, 2004

During the initial finding of ADP-ribosylated substrates, other groups have shown and theorized about unidentified substrates. Coburn et al. and Riese et al. showed ExoS substrates of molecular weights outside of the known substates via Coomassie staining and autoradiography, respectively. Of these unknown substrates, we hypothesize that one or more play a role in caspase-4 mediated cell death, as well as other potential roles in bacterial pathogenesis yet to be identified (8).

Pseudomonas aeruginosa is both an Intracellular and Extracellular Pathogen

P. aeruginosa has been primarily thought to be an extracellular pathogen. This is based on the exoenzyme functions. Cytotoxic strains, encoding ExoU, predominantly act as extracellular pathogens (14). This includes many clinical isolates of *P. aeruginosa*, thus establishing the idea that *P. aeruginosa* is an extracellular pathogen (36, 37). In addition, ExoT also has RhoGAP

activity and is encoded in almost all known T3SS-encoding strains, which is known to keep bacteria extracellular (13, 36). On the other hand, strains that encode ExoS can establish and maintain multiple intracellular niches (38). *P. aeruginosa* was first shown to internalize in human pulmonary carcinoma cells in vitro in 1991 (39). Chi et. al. also found that intracellular bacteria were contained inside intracellular vesicles. Three years later, Fleiszig et. al. showed that *P. aeruginosa* invades corneal cells during in vivo experiments using mice (40). The following year, the same group demonstrated that *P. aeruginosa* can also invade and replicate in cultured primary corneal cells (41). *P. aeruginosa* internalizes into nonphagocytic cells in a manner dependent on phosphoinositide 3-kinase (PI3K): a family of lipid kinases that control adhesion and phagocytosis (42, 43). In the presence of PI3K inhibitors, such as LY294002 and Wortmannin, *P. aeruginosa* internalization has been shown to be significantly reduced (42). The ADP-ribosylation domain of ExoS is also required for bacterial survival and to induce membrane blebs in epithelial cells, which bacteria occupy (7).

During invasion of corneal epithelial cells, *P. aeruginosa* uses its effector toxins to prolong the integrity of invaded cells and maintain a niche (7, 44). When *P. aeruginosa* lacks the effector toxins ExoS, ExoT, and ExoY, there is a significant decrease in how long invaded cells survive (45). When the ADPr domain of ExoS is reintroduced via a plasmid, the survival time of invaded cells is restored back to wild type (wt) levels (7) (Fig. 2A).

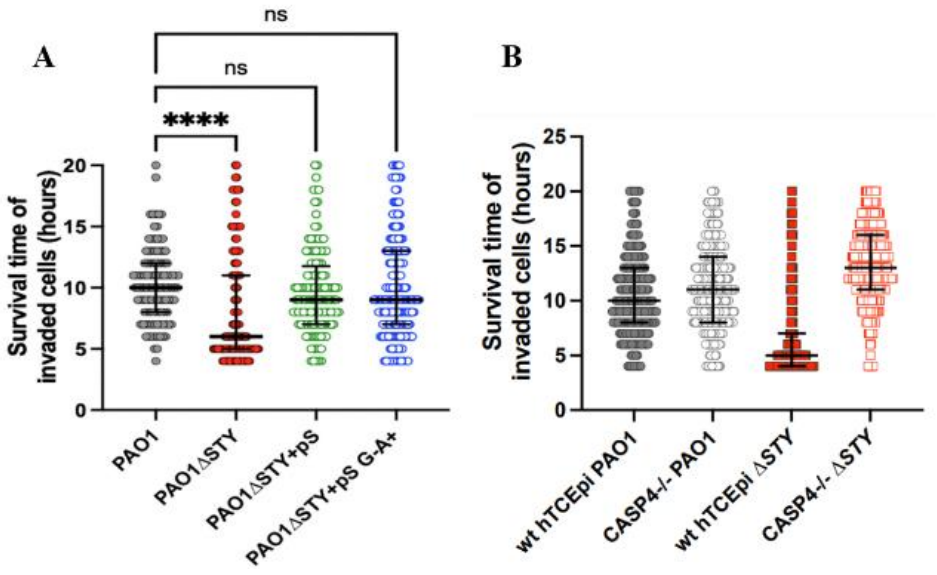

Figure 2. ExoS ADPr Domain Prolongs Invaded Host Cell Life and Likely Interferes with Caspase-4 Mediated Pyroptosis. (A) Corneal epithelial cells were infected with PAO1, PAO1Δ*exoSTY* or PAO1Δ*exoSTY* complemented with ExoS on a plasmid with indicating enzymatic activities for 3hrs. Data from Kroken, A. R., et al 2022 (4). **(B)** Caspase-4 knockout corneal epithelial cells were infected with PAO1 or PAO1Δ*exoSTY* for 3hrs. Unpublished data collected by AR Kroken and KA Klein. Host cell survival data expressed as the median with IQR. Kolmogorov-Smirnov (KS) significance values versus PAO1, * $P < 0.05$, ** $P < 0.01$, **** $P < 0.001$.

Introduction to Host Response of Intracellular Pathogens

Host cells first respond to bacterial infection through innate immunity, to control the pathogenic infection. Host pattern recognition receptors (PRRs) trigger innate immunity by recognizing common pathogenic features. While primarily studied in antigen presenting myeloid cells, PRRs are also expressed in epithelial cells such as corneal and skin cells. PRRs recognize microbes extracellularly by membrane bound Toll-like receptors (TLRs) and intracellularly through NOD-like receptors (NLRs) and inflammatory caspases. Recognition of intracellular pathogenic damage, via NLRs and other intracellular PRRs, leads to the formation of the canonical inflammasome. Each NLR recognizes a specific pathogenic response resulting in inflammasome assembly (46). The inflammasome was first identified as a multiprotein complex of an NLR, a pyrin domain (PYD)-containing protein, an adaptor protein containing a caspase

recruitment domain (CARD), and caspase-1 (47). The multiprotein complex acts as a platform which allows for the cleavage and activation of caspase-1 (48). TLR4 recognizes lipopolysaccharides (LPS) in the outer layer of gram-negative bacteria, including *P. aeruginosa* (49), which allows for the production of inflammatory cytokines, chemokines and proteins.

Intracellular LPS is detected by caspase-4/11 (50, 51) through guanylate-binding proteins (GBPs) that assemble on and coat the outside of gram-negative bacteria (52) by binding LPS (53). This GBP coat allows for the recruitment and activation of caspase-4/11. Active caspase-4/11 can then initiate pyroptosis through the cleavage of full length Gasdermin-D (GSDMD) into GSDMD p30, which goes on to form membrane pores (54). This caspase-4/11 induced pyroptosis is termed the non-canonical inflammasome. Alternatively, active caspase-1 can also cleave GSDMD through the canonical inflammasome (55). Data collected by others in the Kroken lab shows that when caspase-4 is knocked out from host cells, cells invaded by the *P. aeruginosa* mutant lacking exotoxins have increased survival times and permit more bacterial replication (Fig 2B) (8). Since ExoS lacks any known substrates involved in the caspase-4 inflammasome pathway, we decided to identify novel ExoS ADPr substrates as a method to identify how ExoS delays pyroptosis.

Aims and Hypothesis

We hypothesized that among its uncategorized substrates, ExoS ADP-ribosylates a target in the noncanonical inflammasome pathway to delay host cell death. In the course of this study, we also tested whether detecting ADP-ribosylation by immunofluorescence could be used to ask whether *P. aeruginosa* internalization into corneal epithelial cells is needed for T3 secretion and toxin delivery.

In Aim 1, we attempted to characterize the "ADP-ribosyl-ome" of ExoS through mass spectrometry, flow cytometry, immunoprecipitation, and the creation of an ExoS-BirA fusion protein. During the mass spectrometry data collection on whole cell lysates, we noticed that during *P. aeruginosa* infection protein expression is similar to that of *Shigella* infection. The method development for this aim remains ongoing.

In Aim 2, we investigated if a correlation exists between *P. aeruginosa* internalization and whether cells receive ExoS. Results from this aim show that there is a correlation between internalized bacteria and how many cells become ADPr-positive. This correlation differs between the corneal and HeLa cell models. When bacterial internalization is blocked through PI3K inhibitors, no ADP-ribosylation is detected. This approach will be extended to other models and allow us to investigate the relative importance of invasion in bacterial delivery of T3SS toxins.

CHAPTER TWO

MATERIALS AND METHODS

Bacterial Strains and Plasmids

P. aeruginosa strain PAO1 and isogenic T3SS mutants were provided by Dr. Arne Rietsch (Case Western Reserve University) (56).The T3SS-GFP reporter pJNE05 and pUC18 Tn7 $Prha^{exsA}$ plasmids were provided by Dr. Timothy Yahr (Bellin College) (57). Exogenous expression of ExoS and ExoT was accomplished with pUCP18 vectors provided by Dr. Joseph Barbieri (Medical College of Wisconsin). The BirA fusion plasmid PA0709-birA was provided by Dr Andy Ulijasz (Loyola University Chicago).

The ExoS-BirA fusion plasmid was generated by cloning the BirA insert from PA0709-birA into the pUCP18 ExoS backbone. The BirA insert was generated via PCR from primers flanking both the glycine linker region and the FLAG tag. The BirA PCR product was purified using the QIAquick PCR Purification kit (Qiagen). The pUCP18 vector was digested through Sal1 and Kpn1 restriction sites, then recovered using the QIAquick Gel Extraction kit (Qiagen). The vector and insert were ligated together using the Quick Ligation Kit (NEB M2200). The plasmid was heat shocked into DH5α *E. coli* (NEB C2987I) and isolated using the QIAquick Spin miniprepped kit (Qiagen). 50ng of plasmid was then electroporated in *P. aeruginosa* suspended in 300 mM sucrose in a 0.2 cm gap cuvette (BioRad 1652086) for 2 seconds. Bacteria were cultured in LB media for 1 hour before being plated on tryptic soy agar (TSA) plates with antibiotic selection.

Table 2. Strains and Plasmids Used.

Strain or plamsid	Description	Source or reference
Strain		
PAO1	Wild type	Arne Riestch (Case Western Reserve University)
PAO1ΔexsA	exsA mutant	Arne Riestch (Case Western Reserve University)
PAO1ΔexoSTY	exoS, exoT, and exoY mutant	Arne Riestch (Case Western Reserve University)
Plasmid		
pUCP18	P. aeruginosa expression vector	Joseph Barbieri (Medical College of Wisconsin)
pExoS (pUCP18 ExoS-HA)	ExoS expression vector	Joseph Barbieri (Medical College of Wisconsin)
pJNE05	T3SS-GFP reporter	Timothy Yahr (Bellin College)
pUC18 Tn7 $Prha^{exsA}$	Rhammnose inducible T3 expression vector	Timothy Yahr (Bellin College)
pBAD GFP	Arabinose inducible GFP fluorescence vector	Abby Kroken (Loyola University Chicago)

Table 3. List of Primers Used.

Primer Name	Sequence
BirA_Sal1_F	5'-catgtcgtcgacaGGTGGCGGCGGCAGCGGG-3'
BirA_Kpn1_R	5'-ggggatccTCATTTGTCATCATCATCCTTATAGTCGGAGCGCCGC-3'

Cell Culture

HeLa cells were cultured in DMEM (Gibco) plus 10% fetal bovine serum (Avantor). Human telomerase-immortalized corneal epithelial cells (hTCEpi) were provided by Dr. Daniel Robertson (University of Texas Southwestern)(58) and were maintained in KGM-2 media (0.15 mM calcium) (Lonza) in an undifferentiated state. For differentiation, KGM-2 containing 1.15 mM calcium was added to hTCEpi. The corneal cells were seeded at ~ 70% confluence to enhance *P. aeruginosa* internalization via basolateral surfaces.

Infection of Cultured Cells

P. aeruginosa cells were grown as a lawn on TSA containing selective antibiotics overnight at 37°C. Bacteria were suspended in sterile phosphate-buffered saline (PBS) by gentle pipetting. Multiplicities of infection (MOIs) were calculated using an A540 of 1($4X10^8$ CFU). An MOI of 10 was used for all experiments.

Western Blot

Cells were infected with bacteria for 3 hours, then lysed in Pierce IP lysis buffer (pH 7.4, 25mM Tris, 150mM NaCl, 1mM EDTA, 1% NP40, 5% glycerol) (Fisher Scientific PI87787) and Mammalian ProteaseArrest 100X (VWR 78000-036). Nuclei and insoluble material were removed by centrifugation at 4C for 20 minutes at 12000g. Samples were resolved in 4x Laemmli buffer using 4–20% gradient Tris Glycine gels (Bio-Rad 4568095) with stain free label. Total protein was visualized in gel on a Bio-Rad ChemiDoc instrument prior- and post-transfer to PVDF membrane (Bio-Rad 1620177). ADP-ribosylated protein was detected using the rabbit anti-mono-ADP-ribose binding reagent (Sigma-Aldrich mabe1076, 1:6000) in 5% BSA (Fisher Scientific) in TBST (20mM Tris, 150mM NaCl, 0.1% Tween-20, pH 7.5), and secondary goat anti-rabbit HRP (BioRad 1706515, 1:3000). Biotin labelled NAD+ was detected using Pierce High Sensitivity Streptavidin-HRP (Fischer Scientific PI21130, 1:4000) in EveryBlot Blocking Buffer (BioRad 12010020). FLAG tag was detected using mouse Monoclonal ANTI-FLAG M2 antibody (Sigma-Aldrich F3165, 1:10000) in 2.5% milk in TBST, and secondary goat anti-mouse HRP (BioRad 1706515, 1:3000). Clarity Western ECL Substrate (Biorad 1705061) was used to view the HRP secondary.

Immunoprecipitation

Initial attempts at immunoprecipitation were conducted using protein A agarose (Sigma-Aldrich PROTAA-RO) and the mono ADPr binding reagent (Sigma-Aldrich mabe1076). hTCEpi cells were lysed as described previously for western blots and incubated with 1ug or 3ug of the anti-mono-ADPr binding reagent alongside binding buffer (800ul Peirce IP lysis buffer, 1mM DTT) for 3 hours with gentle mixing at 4C. This ADPr binding reagent incubated lysate was then added to binding buffer washed protein A beads and incubated for 3 hours at 4C. The unbound fraction was then collected, and the beads were washed three times with binding buffer. After

boiling in 4x Laemmli sample buffer (BioRad 1610747), samples were run in buffer on 4–20% gradient Tris Glycine gels.

Crosslinked IPs were conducted using a Pierce™ Crosslink Magnetic IP/Co-IP Kit (Fisher Scientific PI88805). 1X Modified Coupling Buffer was preprepared by diluting both IP Lysis/Wash Buffer (pH 7.4, 25mM Tris, 150mM NaCl, 1mM EDTA, 1% NP40, 5% glycerol) and 20X Coupling buffer (10mM sodium phosphate, 150mM NaCl; pH 7.2) into ultrapure water at a 1:10 ratio. This buffer was used to prewash the Pierce Protein A/G Magnetic Beads. 5ug to 10ug of mono ADPr binding was diluted 1:20 with 20X Coupling Buffer and 1:20 with IP Lysis/Wash Buffer, before being incubated on the magnetic protein A/G beads for 15 minutes at room temperature. The magnetic beads were then washed three times using a 1X Modified Coupling Buffer. Bound mono ADPr binding reagent was then crosslinked to the beads using 0.25mM DSS for 30 minutes at room temperature. The beads were first washed three times with Elution Buffer (pH 2.0), and again washed twice with IP Lysis/Wash Buffer. hTCEpi cell lysate was diluted to 500ul using the IP Lysis/Wash Buffer and incubated with the crosslinked beads for 1 hour at room temperature. The unbound fraction was collected, and the beads were washed twice with IP Lysis/Wash Buffer, along with a final ultrapure water wash. The antigen was eluted using the Elution buffer and the pH was neutralized using the Neutralization Buffer (pH 8.5). After boiling in 4x Laemmli sample buffer, samples were run in buffer on 4–20% gradient Tris Glycine gels.

Biotinylated APD Ribosylation Assay

Methods were adapted from Riese et al. (2002) (9). hTCEpi cells were infected at an MOI of 10 for three hours, then cooled down to 4C with cold water at 1:3 ratio with S buffer (130mM sucrose, 50mM KCl, 50mM Potassium acetate, 20mM HEPES pH 7.4) Saponin (Fisher

Scientific AAA1882014) at 75ug/ml was added with cold 1:3 S buffer for 10 minutes at 4C. The saponin solution was removed, and buffer warmed to 37˚C containing 4 uM biotinylated NAD (Tocris 6573) was added, and cells incubated at 37˚C for 40 minutes. Solution was removed and the cells were lysed in RIPA buffer (Sigma-Aldrich R0278). Nuclei and insoluble material were removed by centrifugation 4C for 20 minutes at 12000g. Samples were resolved in 4x Laemmli buffer on 4–20% gradient Tris Glycine gels (Bio-Rad 4568095) with stain free label.

Immunoprecipitation of Biotinylated ExoS Substrates

Lysate from the Biotinylated APD ribosylation assay was diluted with PBS, before being incubated with Pierce NeutrAvidin Agarose (Thermo Fisher Scientific 29201) for 1 hour at 4C. The unbound fraction was collected before the NeutrAvidin beads were washed four times with PBS. After boiling in 4x Laemmli sample buffer (BioRad 1610747), samples were run on buffer on 4–20% gradient Tris Glycine gels.

Fluorescence Activated Cell Sorting (FACS) of Invaded Cells

hTCEpi cells were infected with T3SS inducible *P. aeruginosa* strains, Prha^{exsA} pJNE05, for 3 hours to allow for bacterial internalization. The cells were then treated with 100µL/mL amikacin for 30 min to eliminate extracellular bacteria. 2% Rhamnose was added for three hours to allow for the induction of the T3SS and secretion of ExoS. The cells were then lifted using 0.05% Trypsin-EDTA. Cells were sorted for GFP signal by the FACS core using the FACSAria IIIu. Cells positive for GFP signal were then spun down and given to the proteomics core for analysis.

Mass Spectrometry

Mass spectrometry of ADP-ribosylated substrates were conducted by the proteomics core and in collaboration with the Kirk lab. The following methods were provided by Seby Edassery:

Cell pellets were resuspended in 150 µl of 50mM Tris buffer containing 8M Urea and protease inhibitors. Proteins were extracted by agitating with glass beads at high-speed using TissueLyser LT(Qiagen). SDS and NP40 were added to get a final concentration of 0.1 % detergent each and incubated in ice for 30 min. The protein sample was then purified using chloroform-methanol purification, and the protein precipitate was solubilized in 100 ul of 8 M urea/50 mM Ammonium bicarbonate (ABC), pH 8.0 solution, reduced with five mM DTT for 30 min, and alkylated with 15 mM iodoacetamide for 20 min in the dark. The protein solution was diluted (1:4) with 50mM ABC to reduce the urea concentration and digested overnight at 37 °C with mass spec grade Trypsin (1:50, Thermoscientific 90305). Digestion was stopped with formic acid 0.1% final concentration, centrifuged, and the supernatant was used to purify peptides using C18 spin columns (G-Biosciences 786-931) as per manufacture protocol. Purified peptides were dried using speed vac and resolubilized in 20 ul of 2.5% acetonitrile and 0.1% of FA, 4 ul of resolubilized peptides loaded onto a Vanquish Neo UHPLC system (Thermo Fisher) with a heated trap and elute workflow with a c18 PrepMap, 5mm, trap column(P/N 160454) in a forward-flush configuration connected to a 25cm Easyspray analytical column(P/N ES802A rev2) 2u,100A,75um x 25 with 100% Buffer A (0.1% Formic acid in water) and the column oven operating at 40 °C. Peptides were eluted over a 150 min gradient using 80% acetonitrile, and 0.1% formic acid (buffer B), going from 4 % to 12% over 10 min, to 45% over the next 120 min, then to 99% over 13 min, and then kept at 99% for 7 min, after which all peptides were eluted. Spectra were acquired with an Orbitrap Eclipse Tribrid mass spectrometer with FAIMS Pro interface (Thermo Fisher Scientific) running Tune 3.5 and Xcalibur 4.5. For all acquisition methods, spray voltage set to 1900V, and ion transfer tube temperature set at 300 o C, FAIMS switched between CVs of −45 V, – 55 V, and −65 V with cycle times of 1.5sec. MS1 spectra

were acquired at 120,000 resolutions with a scan range from 375 to 1600 m/z, normalized AGC target of 300%, and maximum injection time of 50ms, S-lens RF level set to 30, without source fragmentation and datatype positive and profile; Precursors were filtered using monoisotopic peak determination set to peptide; included charge states, 2-7 (reject unassigned); dynamic exclusion enabled, with n = 1 for 60s exclusion duration at ten ppm for high and low. DDMS2 scan using isolation mode Quadrupole, Isolation Window (m/z): 1.6; activation Type set to HCD with 30% Collision Energy (CE), IonTrap as a detector with scan rate Turbo, AGC target set to 10,000; maximum Injection Time set to 35ms, micro scans: 1 and data type set to Centroid.

Raw data were analyzed using Proteom Discoveror 2.5 (Thermo Fisher) using Sequest HT search engines. The data were searched against the human Uniprot protein sequence database (Home Sapiens Proteome ID UP000005640). The search parameters included precursor mass tolerance of 10 ppm and 0.06 Da for fragments, allowing two missed trypsin cleavages, oxidation (Met) and acetylation (protein N-term), and Phosphorylation (S, T, Y) as variable modifications, and carbamidomethylation (Cys) as a static modification. Percolator PSM validation was used with the following parameters: strict false discover rate (FDR) of 0.01, relaxed FDR of 0.05, maximum ΔCn of 0.05, and validation based on q-value. Precursor Ions Quantifier settings were to use Unique + Razor for peptides; precursor abundance was based on Intensity, normalization based on total peptide amount, protein abundance was calculated by the summed intensity of connected peptides, and protein ratios were calculated based on protein abundance and a background based T-test was used to calculate statistical significance.

Mass Spectrometry Analysis

Data were analyzed using the Database for Annotation, Visualization, and Integrated Discovery (DAVID) (59, 60). Data were first sorted to have an Abundance Ratio P-Value

(sample/control) of less than 0.05. The negative log P-Value and the fold change (Log2 Ratio) were then calculated using the Abundance Ratio P-Value. Upregulated proteins, Abundance Ratio (sample/control) greater than 1, were uploaded as a gene list into DAVID. The Functional Annotation Tool was then used to find the Biology Process (BP) Gene Ontology (GO) and Kyoto Encyclopedia of Genes and Genomes (KEGG) pathways that were upregulated upon *P. aeruginosa* infection of hTCEpi cells compared to uninfected controls. The Venn diagram comparing the protein expression profile of infections was generated using InteractiVenn.

Immunofluorescence

For Immunofluorescence of the mono ADPr binding reagent, hTCEpi cells were seeded onto glass coverslips, and infected with strains of *P. aeruginosa* containing the fluorescent T3SS reporter plasmid pJNE05. For HeLa cells, coverslips were coated with rat tail collagen I (Thermo Fischer Scientific A1048301) for 1 hour prior to seeding. Cells were infected at an MOI of 10 for 3 hours to allow for bacterial internalization. The cells then were treated with 100µL/mL amikacin for 1 to 2 hours to eliminate extracellular bacteria. Cells were fixed using 4% paraformaldehyde for 10 minutes. The fixation was quenched using 50mM glycine in PBS for 10 minutes. Cells were covered and blocking reagent (5% FBS, 2.5% gelatin, 0.1% TritonX-100, 0.05% Tween-20 in PBS) was added for 1 hour at room temperature. 1ug of mono ADPr binding reagent was added 1:1000 to antibody solution (2.5% FBS, 1.25% gelatin, 0.1% TritonX-100, 0.05% Tween-20 in PBS) and covered overnight at 4C. Cells were washed using PBS, and secondary goat anti-mouse IgG Alexa 555 antibody (Thermo Fisher Scientific, 1:1000) in antibody solution was added at room temperature for an hour. The cells were washed again before DAPI solution in PBS was added for 5 minutes. The cells were washed one time before being mounted onto microscope slides using prolong glass (Fisher Scientific P36982).

For immunofluorescence of the cells treated with PI3K inhibitors, hTCEpi cells were seeded onto glass coverslips. Cells were infected with a strain of *P. aeruginosa* that has a deletion of the main transcription factor for the T3SS, Δ*ExsA*, and with inducible fluorescent plasmid pBAD-GFP. Cells were pretreated with 5mM 3-Methyladenine (InvivoGen inh-3ma-2), 50uM LY294002 (Cell Signaling 9901), or 0.2uM Wortmannin (Cell Signaling 9951) for 1 hour. The pretreated cells were infected at an MOI of 10 for 3 hours to allow for bacterial internalization. The cells were then treated with 100μL/mL amikacin as well as 10% arabinose in KGM2 for 3 hours to eliminate any extracellular bacteria and visualize bacteria. The coverslips were fixed and stained according to the previous immunofluorescence protocol, without the addition of primary and secondary antibody.

Microscopy and Image analysis

Images were captured on a Nikon Ti2-E with X-Cite XYLIS Broad Spectrum LED Illumination System using a CFI Plan Apo Lambda 40X NA 0.95 or 60x CFI Plan Apo Lambda 60X oil objective. ADP-ribose signal was quantified using ImageJ. First, the nuclei were thresholded from background signal and segmented (Fig 3B). The selection area of each nucleus was expanded to include perinuclear cytoplasm (Fig 3C). Then the mono ADPr signal was mapped back to the corresponding nucleus and quantified as the mean intensity per cell (Fig 3 D and E).

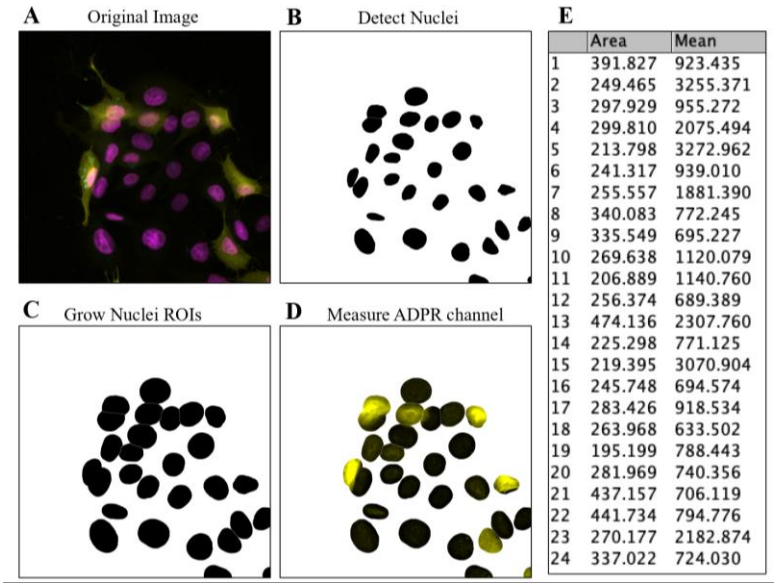

	Area	Mean
1	391.827	923.435
2	249.465	3255.371
3	297.929	955.272
4	299.810	2075.494
5	213.798	3272.962
6	241.317	939.010
7	255.557	1881.390
8	340.083	772.245
9	335.549	695.227
10	269.638	1120.079
11	206.889	1140.760
12	256.374	689.389
13	474.136	2307.760
14	225.298	771.125
15	219.395	3070.904
16	245.748	694.574
17	283.426	918.534
18	263.968	633.502
19	195.199	788.443
20	281.969	740.356
21	437.157	706.119
22	441.734	794.776
23	270.177	2182.874
24	337.022	724.030

Figure 3. Visualization of Intensity Quantification. For each image captured **(A),** nuclei were detected and thresholded from the background **(B)**. Individual nuclei were assigned as a region of interest (ROI), and each ROI was expanded to include the perinuclear cytoplasm **(C).** Mean signal intensity from the ADPr was then determined for each ROI **(D, E).**

Statistics

Statistical analyses were performed, and data presented using Graph Pad Prism 9. Data were shown as a mean ± standard deviation (SD) of at least three independent experiments unless otherwise indicated. For host cell survival data, non-parametric data were shown as a median with inter-quartile range (IQR) for each group. A non-parametric Kolmogorov Smirnov (KS) test was performed against the PAO1 condition for complementation experiments. For immunofluorescence of the mono ADPr binding reagent, fluorescence intensity of each nucleus expressed as the mean with SD. Unpaired t test with Welch's coefficient was used to determine significance. In each instance, * $P < 0.05$, ** $P < 0.01$, **** $P < 0.001$.

CHAPTER THREE

AIM ONE RESULTS

Immunoprecipitation Approaches to Enrich ADP-ribosylated Proteins

Our first approach was to capture total ExoS substrates using immunoprecipitation. ExoS substrates were captured using a commercially available mono ADPr binding reagent. This reagent, described by Gibson, B. A., et al 2017, is a recombinant protein made from the fusion of macrodomain 2 and 3 from mammalian PARP14 to the Fc region of rabbit IgG (61). This reagent was first confirmed to recognize mono-ADP ribosylated proteins via western blotting. Corneal epithelial cells were infected with wt PAO1 (expresses ExoS, T, and Y) or a mutant missing all three toxins or left uninfected (Fig. 4B). Lysates were collected at 4 hours and total protein is shown as a loading control (Fig. 4A).

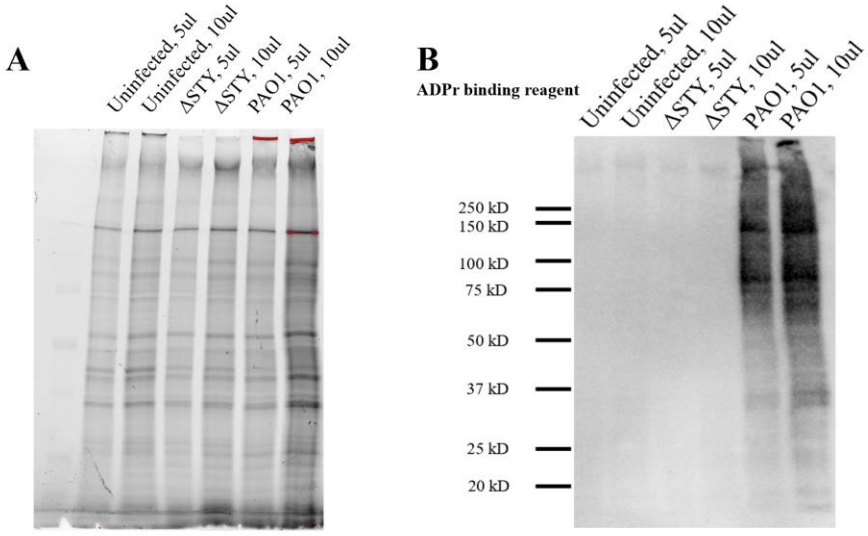

Figure 4. Detection of Potential ExoS Substrates using the mono ADP-ribosylation Binding Reagent. (A) total protein gel and (**B)**immunoblot of lysed cells infected with ΔTY or Δ STY P. aeruginosa using the mono ADPr binding reagent.

We then adapted the mono ADPr binding protein for immunoprecipitation (IP). The ADPr binding protein was bound to protein A/G beads first, and then incubated with lysate from cells infected with either Δ*exoTY* (only expresses ExoS) or Δ*exoSTY* (expresses no toxins). There were no detected substrates in the elution (Fig. 5A and B). Thus, we attempted several types of optimizations. These optimizations included a change in IP methods, from a pre-immobilized antibody approach to a free antibody approach, and the addition of 1mM DTT. Potential substrates were pulled down when the reducing agent DTT was added, but addition of DTT also resulted in the detection of ADP-ribosylated proteins eluted in Δ*exoSTY* negative control, despite no proteins present in the input (Fig. 5C and D). This was attributed to the ADPr binding reagent dissociating from the agarose beads into the elution, because when run on its own, a smear is detected above 150 kDa (Fig. 6A and B, lane 1). To solve this problem, DSS was used to covalently crosslink the binding reagent to magnetic protein A/G beads. While this did solve the issue of detecting mono ADPr binding protein in the elution, no ADP ribosylated substrates were obtained in the elution (Fig. 7A and B). Additional efforts were made to optimize, including increasing the amount of protein A/G breads and mono ADPr binding reagent used; however, there was no improvement.

We investigated the size and stability of the mono ADPr binding protein. In the initial paper describing the reagent, the mono ADPr binding protein ran on a Coomassie gel at 100 kDa, with degradation products detected between 75 and 50 kDa (61). This differed from what we saw when visualizing the reagent during IP attempts (Fig. 6B, lane 1). We then ran boiled and unboiled ADPr binding protein in 4% sample buffer on a gel by itself. Neither method of preparation resulted in the detection of ADPr binding protein at its known size (Fig. 8A and B),

suggesting the binding protein may be unstable. In sum, the mono ADPr binding reagent appears unsuitable for immunoprecipitation in our hands, possibly due to stability and reagent quality.

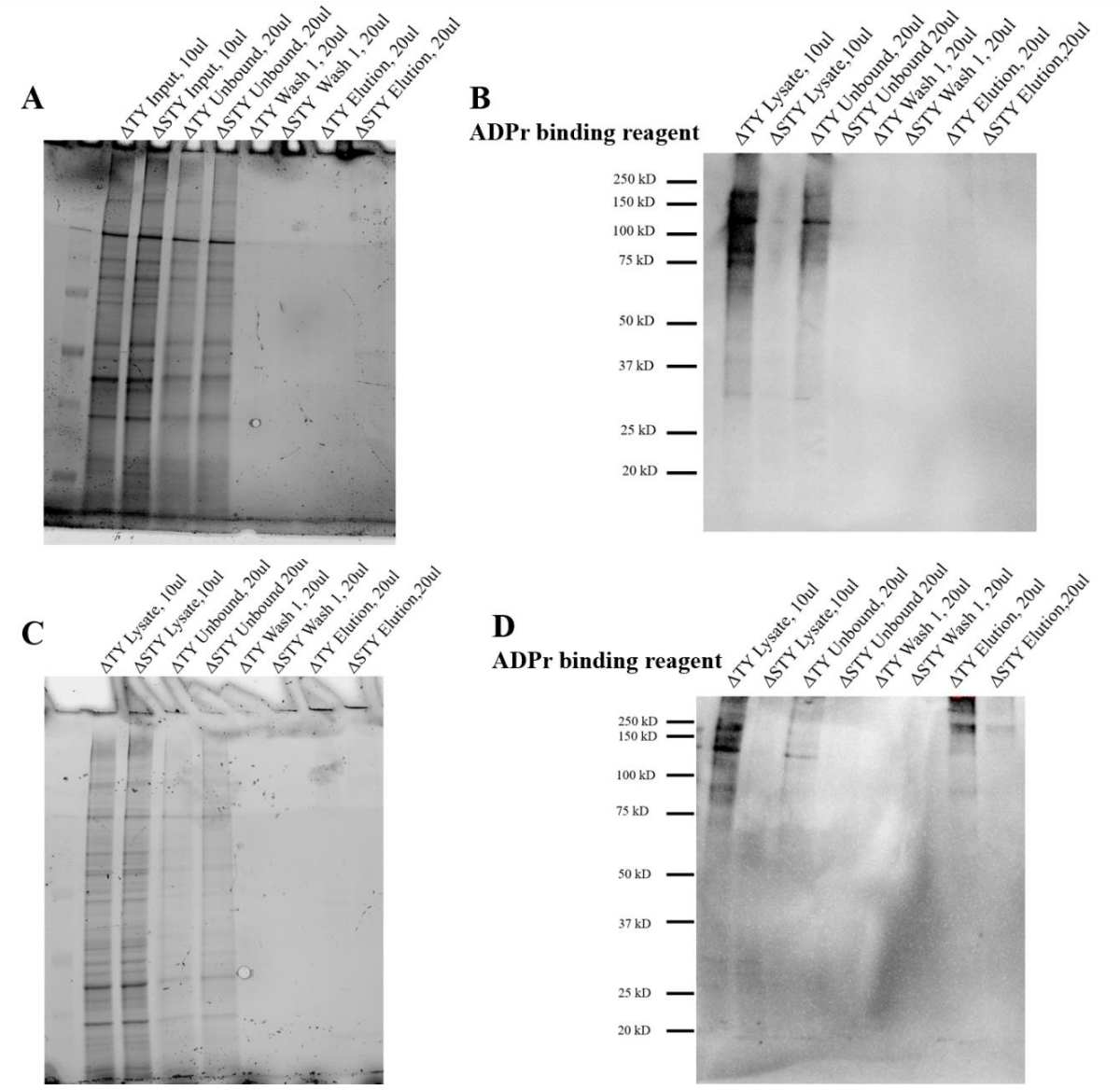

Figure 5. Initial Immunoprecipitation Attempts of Potential ExoS Substrates Using a mono ADP-ribosylation Binding Reagent. (A) total protein gel and **(B)** blot of the first immunoprecipitation using the binding reagent for protein collection and detection. **(C)** total protein gel and **(D)** blot of the optimized immunoprecipitation using the binding reagent for protein collection and detection.

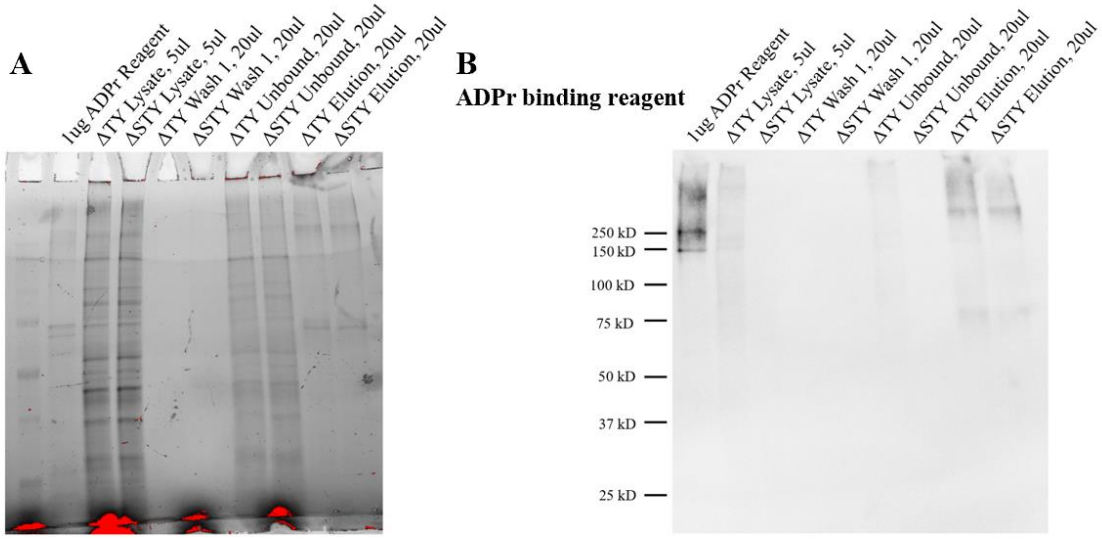

Figure 6. The mono ADPr Binding Reagent is Detected in the Elution. (A) total protein gel and **(B)** blot of Immunoprecipitation using the binding reagent for protein collection and detection. The ADPr binding reagent was detected in the elution.

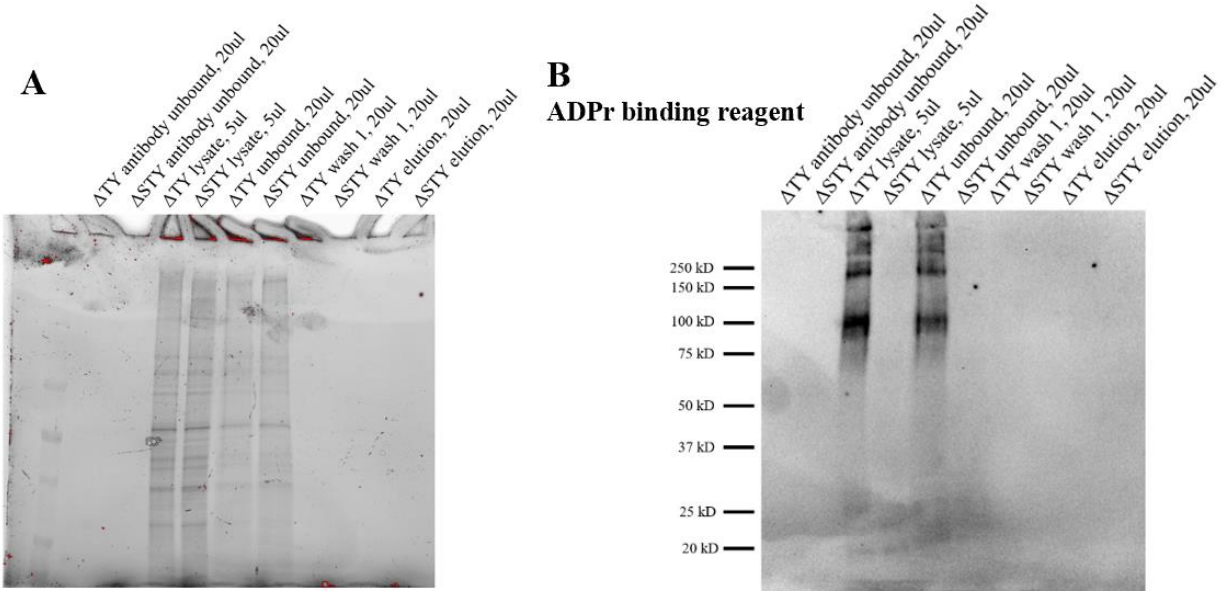

Figure 7. Crosslinking the mono ADPr Binding Reagent to Magnetic Protein A/G Beads Did Not Result in Any Elution. (A) total protein gel and **(B)** blot of the DSS crosslinked immunoprecipitation using the binding reagent for protein collection and detection. Crosslinking the ADPr binding reagent to protein A/G did not result in eluted protein.

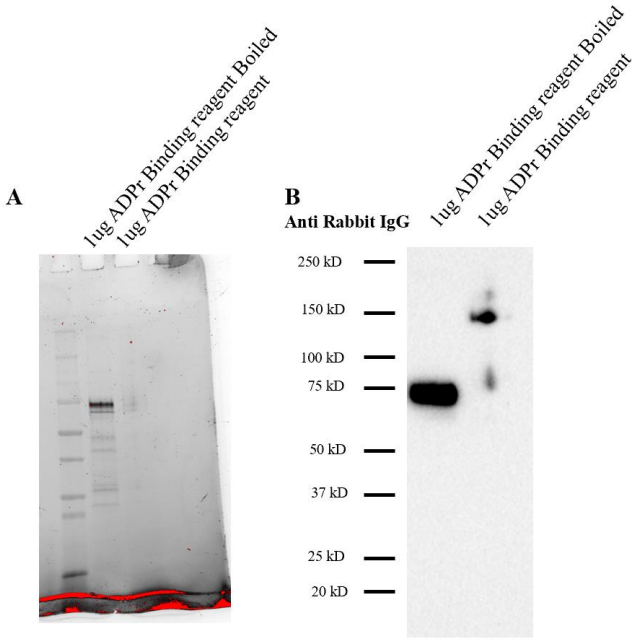

Figure 8. The mono ADPr Binding Reagent is Unsuitable for Immunoprecipitation. (A) 1 ug of the ADPr binding reagent ran on a total protein gel and **(B)** immunoblot of using antirabbit IgG. The ADPr binding reagent appears to be degraded, as it runs at a different size than the literature described (61).

An alternative method to detect ExoS substrates was to pulse in biotin-labeled NAD+ and perform immunoprecipitation for the biotin label using neutravidin beads. This method originally used the pore-forming reagent tetanolysin to permeabilize the cell membrane (9). Unfortunately, tetanolysin is no longer commercially available. Saponin, a plant derived surfactant, along with hypotonic buffer was shown to be a decent alternative to pulse biotinylated-NAD+ into HeLa cells via blotting with HRP conjugated streptavidin, as bands were detected in an ExoS-dependent manner (Fig. 9A). One downside of this method is a dominant nonspecific band independent of ExoS (Fig. 9A). When immunoprecipitating biotin using neutravidin beads, only this nonspecific band was detected in the elution (Fig 9B). Protocol modifications to detergent and bead quantity did not improve results. Considering the protein profile is different using this

method than when we used mono ADPr binding protein (Fig. 9A), we had additional concerns that a subset of substrates may be unable to accept a biotin-ADPr moiety.

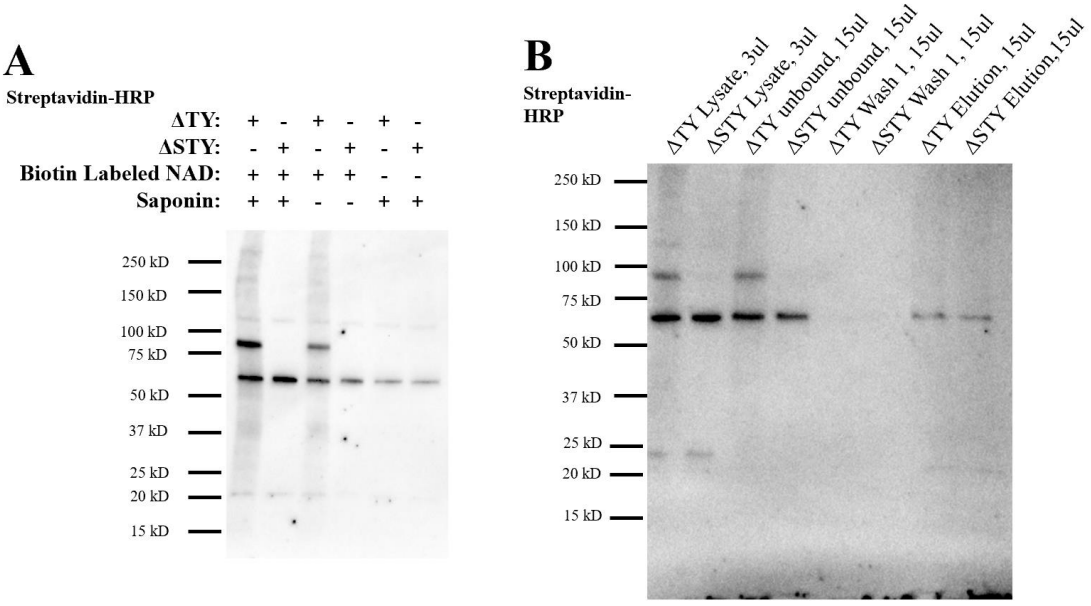

Figure 9. Detection and Immunoprecipitation of Potential ExoS Substrates using Biotin-labelled NAD. (A) Biotin-labelled NAD and/or the pore forming toxin saponin were added to corneal epithelial cells, which were then infected with Δ*exoTY* or Δ*exoSTY P. aeruginosa*. Lysates were collected and used to immunoblot for the biotin label. **(B)** Immunoprecipitation was performed using streptavidin beads.

Total Protein and Enriched Mass Spectrometry

We elected to run total protein lysates without enrichment for ADP-ribosylated proteins in an attempt to detect post translational modifications among the total proteome. Corneal cells were infected with Δ*exoTY* or Δ*exoSTY P. aeruginosa* for 4 hours, and lysates collected. Mass spectrometry was run in collaboration with the Kirk lab and performed by Seby Edassery. After the preliminary round of mass spectrometry, a total of 5,641 proteins were identified. Nine proteins were detected with ADP ribosyl modification on arginine residues; however, none were known ExoS substates (Table 4). If any ExoS substrates were detected, we expected to only find

modification in the Δ*exoTY* infection. Additionally of the nine proteins identified, two proteins, 28 ribosomal protein S11 and YLP motif-containing protein 1, were found to have ADP ribosyl modifications in both Δ*exoTY* and Δ*exoSTY* infections, while another protein only had modification upon Δ*exoSTY* infection. This suggests that only background signal was detected via mass spectrometry. Overall, these results suggest that enrichment for the ADP ribosyl modification is required prior to mass spectrometry.

Table 4. ADP Ribosylated Proteins Identified by Preliminary Mass Spectrometry on Total Cell Lysates. Proteins highlighted in green were highly ADP-ribosylated upon both Δ*exoTY* and Δ*exoSTY* infections. Proteins highlighted in orange were highly ADP-ribosylated upon Δ*exoSTY* infection.

Proteins identified with ADP-Ribosyl Modification
Terminal uridylyl transferase 4
Protein BTG4 (Fragment)
2-C-methyl-D-erythritol 4-phosphate cytidylyltransferase
Myosin-13
Non-homologous end joining factor IFFO1
Transmembrane protein 59-like
28S ribosomal protein S11
Ras-associating and dilute domain-containing protein
YLP motif-containing protein 1

One reason ADP ribosylated proteins may be difficult to detect is that many cells remain unintoxicated by ExoS during infection. Thus, unmodified substrates might outnumber the ExoS modified protein. We decided to enrich cells with internalized *P. aeruginosa* first through FACS sorting. We first asked if corneal cells infected with the T3SS reporter pJEN05 could be sorted for GFP fluorescence when compared to wild type infected or uninfected cells. When collecting intact cells, we observed that corneal cells infected with *P. aeruginosa* are not as effectively trypsinized, when compared to uninfected cells. Infected cells took longer to lift, over 15 minutes

rather than 7 minutes, with only 50% of cells being lifted. Despite this, corneal cells infected with fluorescence *P. aeruginosa* (Fig. 10C) were suitable for FACS sorting (Fig. 10A and B).

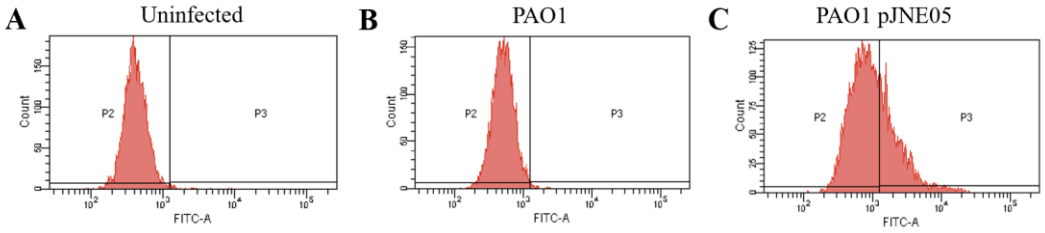

Figure 10. FACS Sorting of Corneal Epithelial Cells. Corneal epithelial cells infected with fluorescent *P. aeruginosa* **(C)** were able to be sorted from uninfected **(A)** and wild type *P. aeruginosa* **(B)**.

To increase the number of sortable cells, we decided to maximize the odds of bacterial internalization. This was done by first infecting corneal cells with *P. aeruginosa* containing a plasmid inducible T3SS. This rhamnose-inducible *exsA* construct, the master transcription factor of T3SS, has been shown to mimic wild type *P. aeruginosa* infection in Δ*exsA* strains (6). Corneal cells were infected with the T3 inducible fluorescent *P. aeruginosa* or T3 inducible fluorescent Δ*exoSTY P. aeruginosa* for a total of six and a half hours. Once the bacteria were intracellular and extracellular bacteria were killed with amikacin, media containing rhamnose was added for three hours to trigger T3 secretion. Corneal cells were then sorted for GFP signal. Around 900,000 total cells were sorted for each infection (Table 5). 17 to 20% of the cells were sorted for intracellular *P. aeruginosa* via GFP signal. Cells positive for GFP signal, along with an uninfected control, were then given to Seby Edassery for sample preparation and mass spectrometry.

Table 5. FACS Sorting of Corneal Epithelial Cells Infected with Type Three Inducible *P. aeruginosa.*

	# GFP Negative Cells	# GFP Positive Cells	Total Cells #	% GFP Positive Cells
Δ*ExsA* Prha^{ExsA} pJNE05	720708	151688	872396	17
Δ*STY* Δ*ExsA* Prha^{ExsA} pJNE05	710886	172735	883621	20

Mass spectrometry of corneal cells enriched for intracellular *P. aeruginosa* was performed by Seby Edassery. After enrichment, a total of 4,700 proteins were identified. Unfortunately, only ten proteins were found to be ADP-ribosylated on arginine residues (Table 6), without any of the proteins being known ExoS ADPr substrates. None of the newly identified proteins were detected in the preliminary mass spectrometry. Eight of the ten identified proteins were found in the uninfected control sample, with the tenth being found only in the *ΔSTY ΔexsA* Prha^{ExsA} pJNE05 negative control infection. Overall, this suggests that again only background signal was detected. Despite some enrichment for intracellular *P. aeruginosa* using FACS, a greater form of enrichment is required prior to mass spectrometry.

Table 6. ADP Ribosylated Proteins Identified by FACS Sorting for Internalize *P. aeruginosa.* Proteins highlighted in green were highly ADP-ribosylated in both infections and the uninfected sample. Proteins highlighted in yellow were only ADP-ribosylated in the uninfected sample. Proteins highlighted in orange were highly ADP-ribosylated in only Δ*exoSTY ΔExsA* Prha^{ExsA} infection.

Proteins identified with ADP-Ribosyl Modification
TATA element modulatory factor
Rab GDP dissociation inhibitor alpha
Cadherin EGF LAG seven-pass G-type receptor 3
Protein FAM171A1
Neutral amino acid transporter A
Annexin A2
TBC1 domain family member 2B
Protein S100-A11
Rab GDP dissociation inhibitor beta
Putative uncharacterized protein encoded by LINC00869

Cloning ExoS-BirA fusion to investigate ExoS interactome

Another strategy for enrichment for ExoS substrates was attempted through the creation of an ExoS-BirA fusion protein for Bio-Id. This system would allow for the identification of substrates

by using a promiscuous biotin ligase, BirA, that biotinylates nearby proteins (62)**Error! Bookmark not defined.**. By fusing BirA to ExoS, any proteins that ExoS interacts with would also be biotinylated. While we were successful in cloning a plasmid containing an ExoS-BirA fusion, the resulting fusion protein was not able to be expressed (Fig. 11A). We were unable to detect the FLAG tagged fusion protein in control or T3SS inducing media, finding only background bands equivalent in negative control samples (Fig. 11B). This was unexpected as ExoS fusion proteins have been made prior (63, 64). In the future, we might consider expressing this construct in mammalian cells directly.

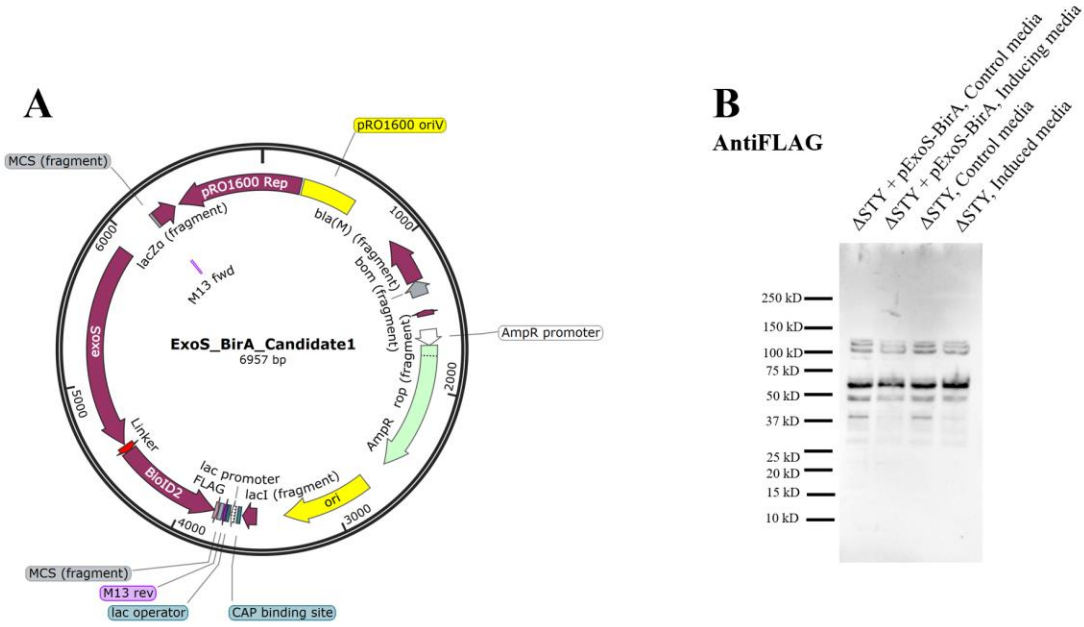

Figure 11: Creation and Expression of an ExoS-BirA Fusion Protein. (A) Sequence of created fusion plasmid. **(B)** Immunoblot of FLAG tagged proteins from ΔSTY *P. aeruginosa* either containing or lacking the fusion plasmid.

Analysis of Mass Spectrometry Results

After conducting mass spectrometry on corneal cells enriched for intracellular *P. aeruginosa*, we analyzed how protein expression changes during infection when compared to the uninfected

control. In corneal cells infected with a strain of *P. aeruginosa* containing ExoS, several protein expression pathways were upregulated (Fig 12A). Moreover, epigenetic histone markers of DNA expression, such as H2A2 and H2AX, were found to be highly upregulated upon *P. aeruginosa* infection (Fig 12A, and E). Additional proteins involved in membrane ruffling and actin polymerization were upregulated in a manner like that of *Shigella* infection (Fig 12B). This upregulation includes the Arp2/3 complex, as well as some upstream proteins, that is required for *Shigella* actin-based motility (65). While *P. aeruginosa* uses a different mechanism, for intracellular motility (66), some of the proteins upregulated in *Shigella* actin-based motility are also involved in immune responses (67). During *P. aeruginosa* infection, some metabolic processes and signaling pathways are down-regulated (Fig. 12 C and D).

Corneal cells responded similarly to the ExoS infection when infected with *P. aeruginosa* lacking ExoS (Fig. 13A, B, and E). When comparing the gene ontology of the corneal cells infected with or without ExoS, protein expression does not drastically differ. However, during both infection conditions, protein expression was similar to a shigellosis infection. Upregulated proteins include Actin, the Arp2/3 complex, as well as Crk and Cortactin which have been shown to trigger actin polymerization upon *Shigella* infection (68). Upon *P. aeruginosa* infection, some proteins involved in metabolic processes were downregulated (Fig. 13C and D). These data further reinforce the intracellular nature of *P. aeruginosa*, demonstrating that *P. aeruginosa* infection changes protein expression in an equivalent manner to other intracellular pathogens.

When comparing protein expression between the two infections, protein translation is upregulated upon both infections (Fig. 14). However, the location of translation varies between infections. In the Δ*exoSTY* infection, endoplasmic translation is mostly highly upregulated (Fig.

14C). This differs in *P. aeruginosa* containing ExoS infection, as cytoplasmic translation is the most upregulated (Fig. 14A).

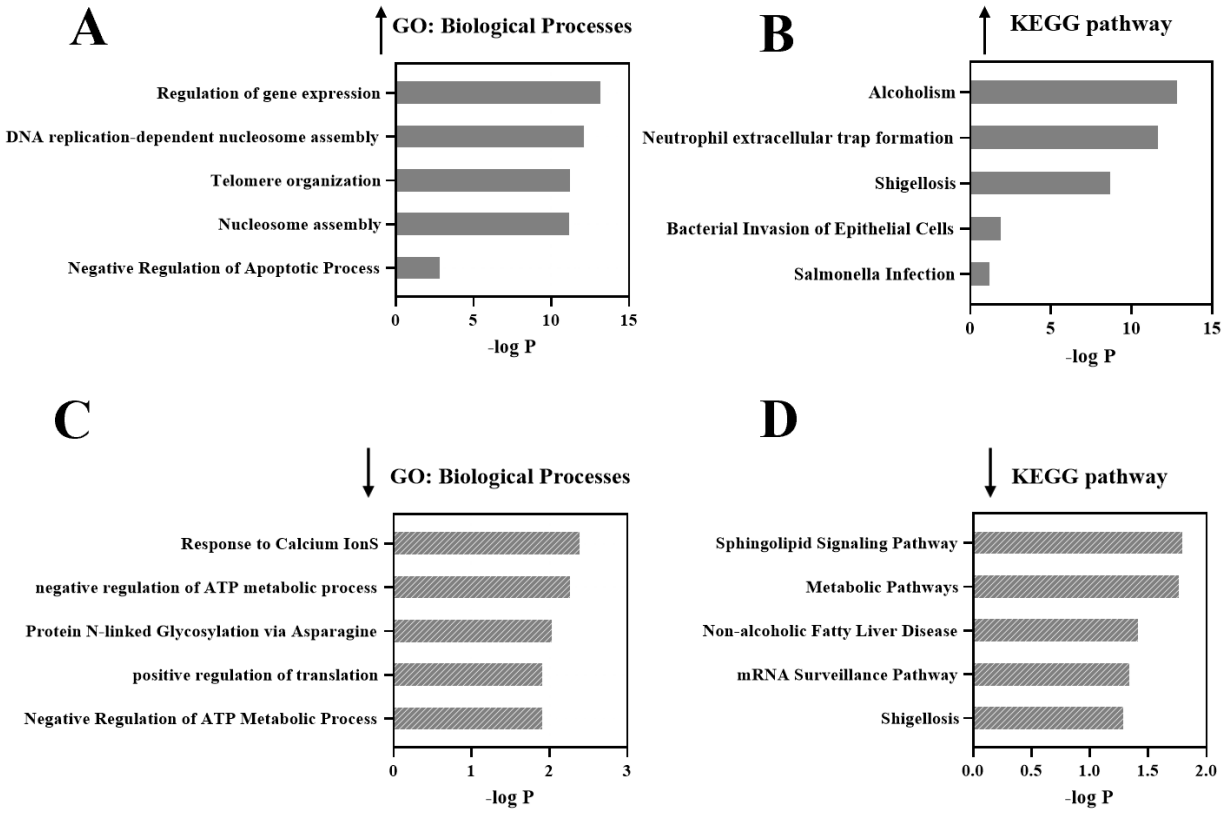

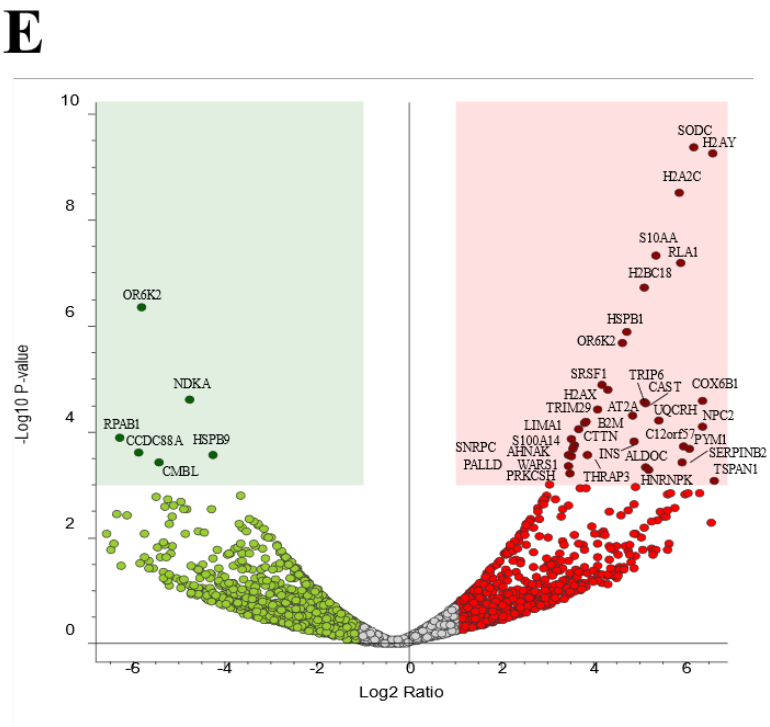

Figure 12: Corneal Cell Protein Expression Changes upon ExoS *P. aeruginosa* Infection. (A) GO terms and **(B)** pathways upregulated upon infection. (**C)** GO terms and **(D)** pathways downregulated upon infection. **(E)** annotated volcano plot.

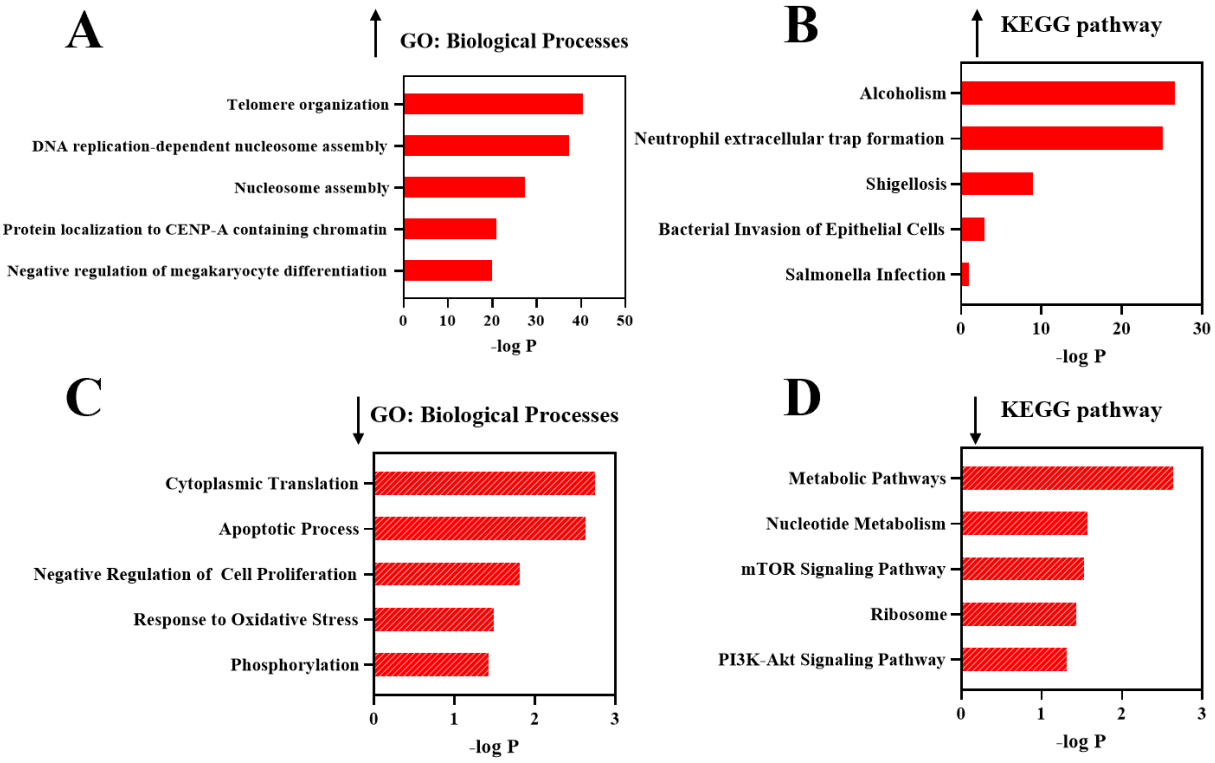

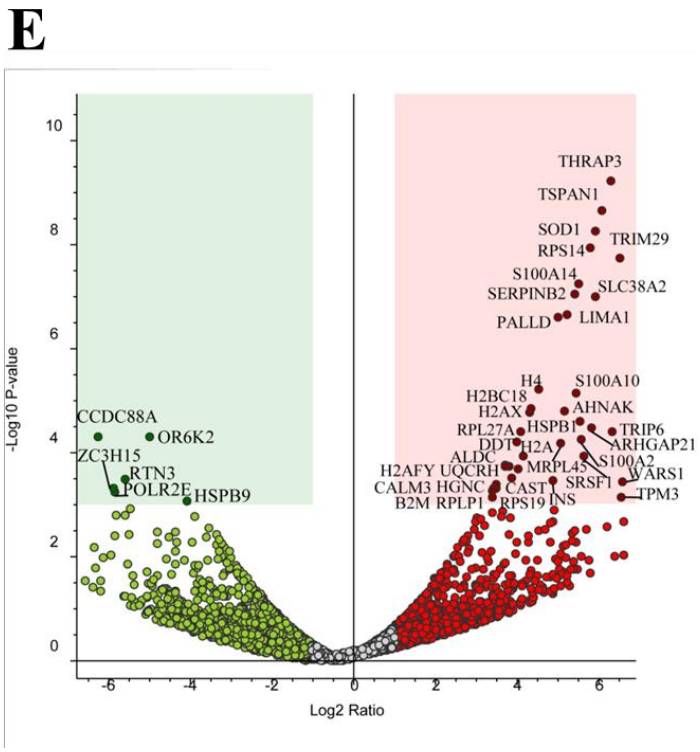

Figure 13: Corneal Cell Protein Expression Changes upon ΔSTY *P. aeruginosa* Infection. (A) GO terms and **(B)** pathways upregulated upon infection. (**C)** GO terms and **(D)** pathways downregulated upon infection. **(E)** annotated volcano plot.

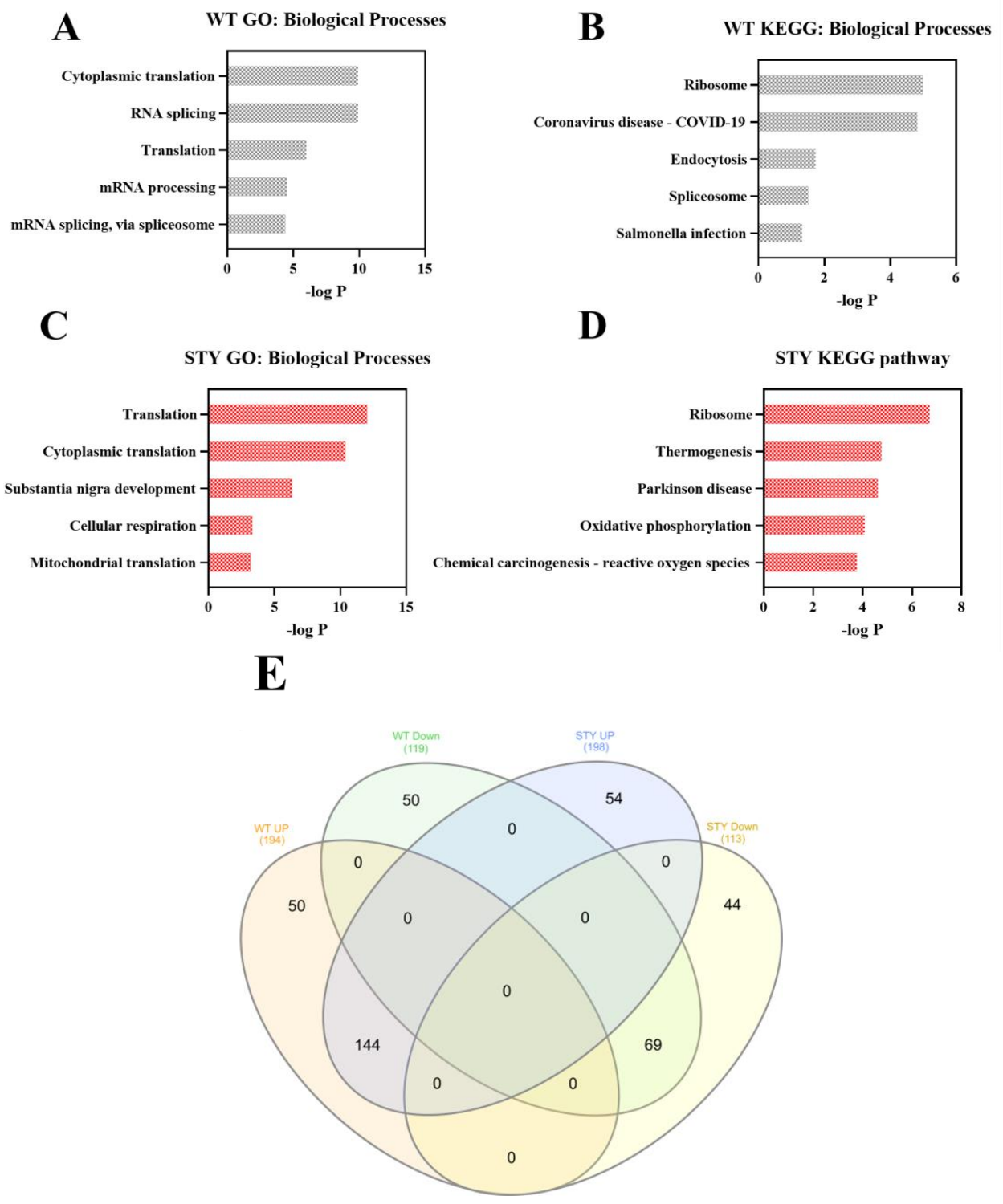

Figure 14: Corneal Cell Protein Expression varies upon ExoS *P. aeruginosa* and ΔSTY *P. aeruginosa* Infections. (A) GO terms and **(B)** pathways upregulated upon induced wild-type infection. (**C)** GO terms and **(D)** pathways upregulated upon induced Δ*exoSTY* infection. **(E)** Venn diagram comparing protein profile of both infections.

CHAPTER FOUR

AIM TWO RESULTS

While characterizing the utility of the mono ADPr binding reagent, immunofluorescence of infected corneal epithelial cells was performed using this reagent as a primary probe. Corneal epithelial cells were grown on coverslips and infected with strains of *P. aeruginosa* containing a fluorescent T3SS plasmid. Surprisingly, an intense signal was detected in a subset of cells, only when corneal cells with *P. aeruginosa* expressing ExoS (Fig. 15). This ADP-ribose signal was quantified using ImageJ to measure how many cells had mono ADPr signal (see methods for a description of the analysis macro). The percentage of cells positive for ADPr signal varies between 18 and 54% (Table 7). This variance is biologically relevant as *P. aeruginosa* preferentially invades the basolateral side of polarized epithelial cells (69). Additionally, the ADPr signal is visually associated with *P. aeruginosa* inside corneal epithelial cells. Noticeably, the number of cells positive for ADPr signal was increased to almost the entire population when staining HeLa cells, a cell line widely used by earlier *P. aeruginosa* researchers and consistent with their prior findings based on cell rounding (70) (Fig. 16). These results were consistent over multiple experiments (Table 7).

Table 7. The percentage of Cells Positive for ADP-ribose Signal was Consist Across Experiments.

	Total Cell Count	Number of Cells Positive for ADP-ribose signal	Percentage
hTCEpi	255	49	19
	201	110	54
	429	77	18
	802	426	53
	821	241	29
HeLa	62	61	98
	362	337	93

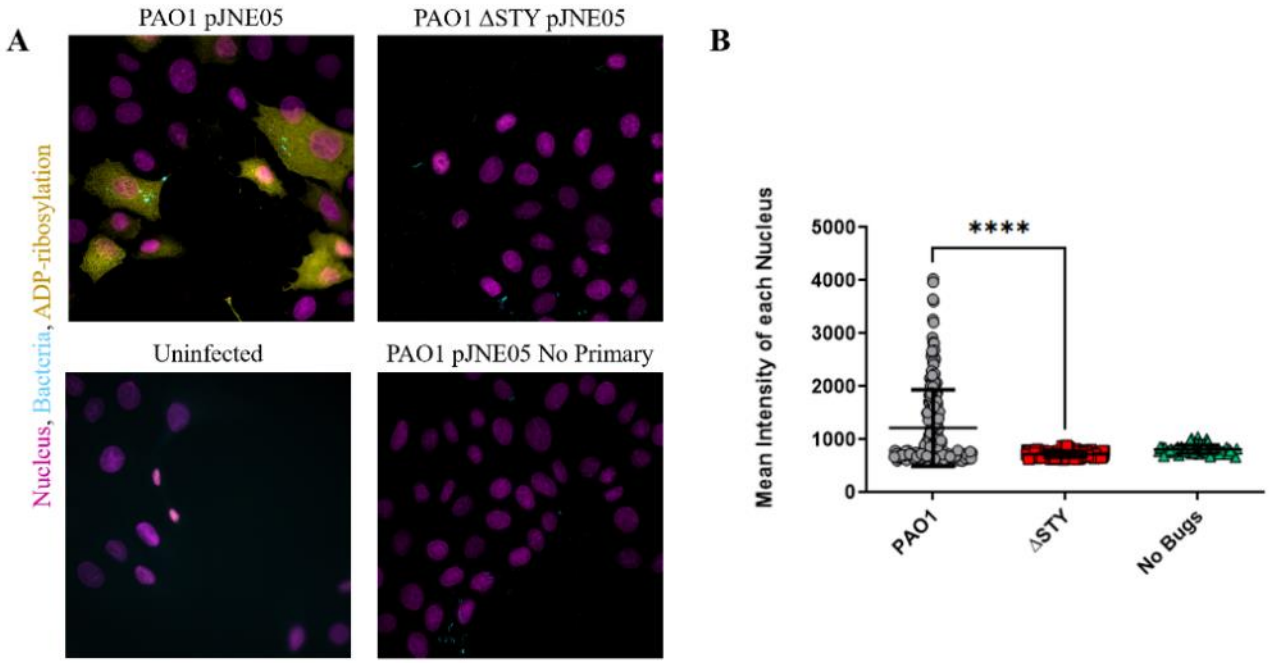

Figure 15. Detection of Potential ExoS Substrates via Immunofluorescence of mono ADP-ribosylation Binding Reagent. (A) 60x Fluorescence microscopy of corneal epithelial cells infected with *P. aeruginosa* (cyan) for 3hr. The cells then were treated with 100µL/mL amikacin for 30 min. ADP-ribosylation (yellow) was visualized by immunostaining with the mono ADPr binding reagent. Nuclei were stained with DAPI (magenta). **(B)** Mean intensity of ADP-ribosylation signal for each nucleus was determined in ImageJ. **** P<0.001, Unpaired t test with Welch's coefficient.

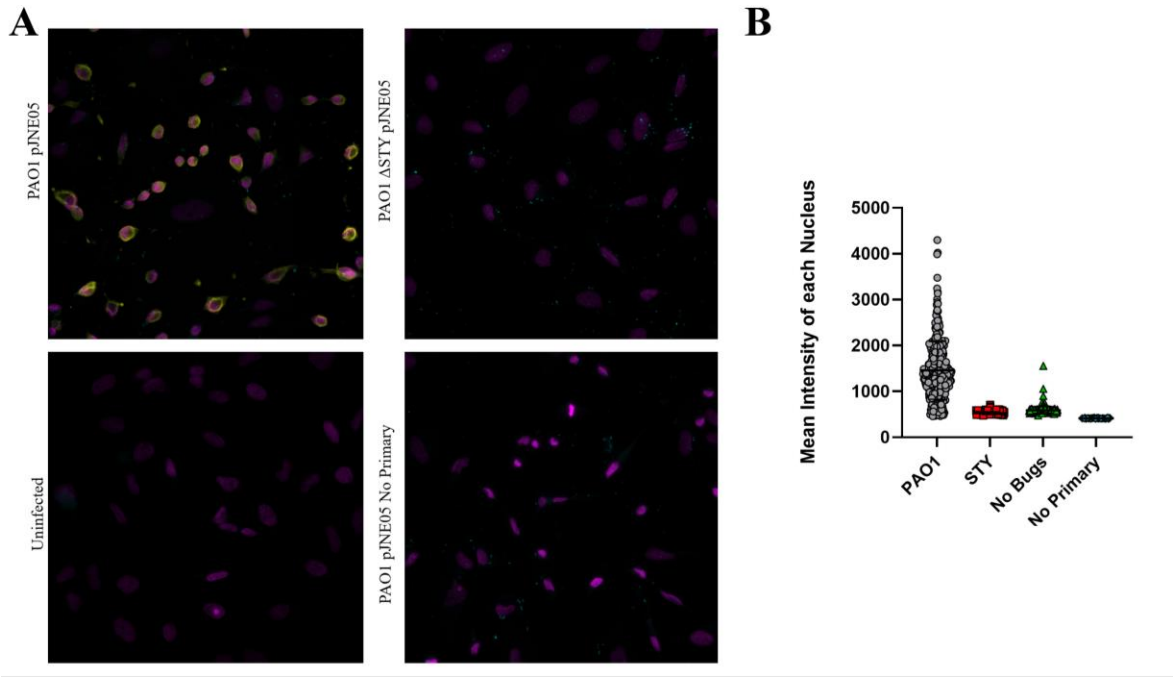

Figure 16: Detection of Potential ExoS Substrates via Immunofluorescence of mono ADP-ribosylation Binding Reagent in HeLa Cells. 40x Fluorescence microscopy of corneal epithelial cells infected with *P. aeruginosa* (cyan) for 3hr. The cells then were treated with 100µL/mL amikacin for 1 hour. ADP-ribosylation (yellow) was visualized by immunostaining with the mono ADPr binding reagent. Nuclei were stained with DAPI (magenta). **(B)** Mean intensity of ADP-ribosylation signal for each nucleus was determined in ImageJ.

The importance of intracellular *P. aeruginosa* during infection is not well understood. Immunofluorescence of the mono ADPr binding reagent has provided a new way to study the frequency of intracellular T3SS intoxication vs invasion by *P. aeruginosa*. To better understand the role of intracellular T3 secretion, we tested if intracellular *P. aeruginosa* is required for ExoS intoxication. To do so, we first treated corneal epithelial cells with the known PI3K inhibitor, inhibitor 3-Methyladedine (3MA), previously shown to block *P. aeruginosa* internalization (42, 43). To visualize intracellular *P. aeruginosa*, we infected cells with Δ*exsA* pBAD GFP, a strain lacking the main T3SS transcription factor that become trapped within cellular vacuoles and can be easily observed with arabinose induction of GFP. We observed that upon 3MA treatment, the number of intracellular bacteria was reduced (Fig. 17). We next tested if inhibition of *P. aeruginosa* internalization would reduce the number of cells positive for ADPr signal. By

pretreating corneal cells with 3-Methyladenine (3MA), a PI3K inhibitor, we saw a complete lack of ADPr signal (Fig. 18), suggesting that bacterial internalization is necessary for ExoS intoxication.

While performing immunofluorescence of the mono ADPr binding reagent, we noticed that cells positive for ADP ribose signal usually contained intracellular *P. aeruginosa.* By hand counting, we determine that 50% of corneal cells positive for ADP-ribose signal contained intracellular *P. aeruginosa* (n=2). While we have demonstrated that cellular ExoS intoxication can be used to identify intracellular *P. aeruginosa* in vitro, we want to see if this relationship is maintained in mouse cornea in future experiments.

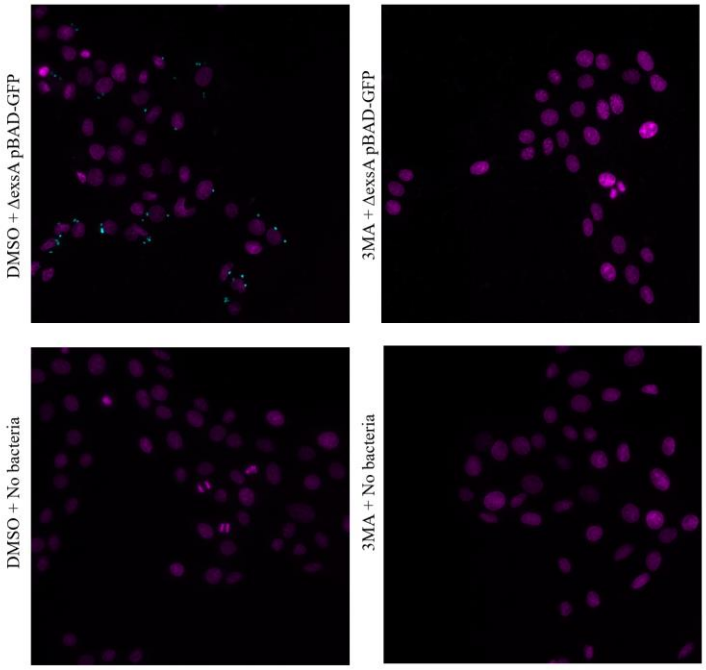

Figure 17: Treatment of 3-Methyladenine Reduces the Number of Intracellular *P. aeruginosa* via Immunofluorescence. Fluorescence microscopy of corneal epithelial cells pretreated with 5mM 3MA for 1hr. Cells were infected with *P. aeruginosa* (cyan) for 3hr. The cells were treated with 100μL/mL amikacin and 10% arabinose for 2 hours. Nuclei were stained with DAPI (magenta).

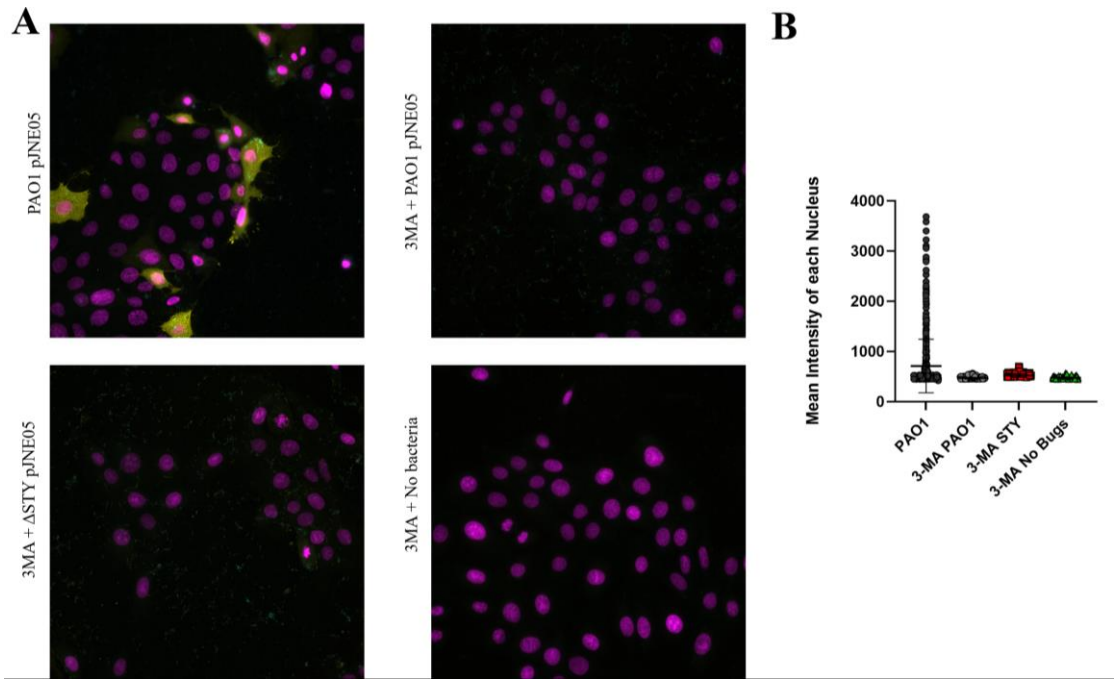

Figure 18: Treatment of 3-Methyladenine Diminishes ADP-ribosylation Signal via Immunofluorescence. Fluorescence microscopy of corneal epithelial cells pretreated with 5mM 3MA for 1hr. Cells were infected with *P. aeruginosa* (cyan) for 3hr. The cells were treated with 100µL/mL amikacin for 2 hours. ADP-ribosylation (yellow) was visualized by immunostaining with the mono ADPr binding reagent. Nuclei were stained with DAPI (magenta). **(B)** Mean intensity of ADP-ribosylation signal for each nucleus was determined in ImageJ

CHAPTER FIVE

DISSCUSSION

P. aeruginosa uses its T3SS to delay host corneal epithelial cell death in an ExoS ADP-ribosyl transferase dependent manner. In *caspase-4* KO corneal cells, ExoS is not required to delay cell death. Of the known ExoS ADP-ribosylation substrates, none are known to be involved in caspase-4 mediated pyroptosis. This suggests a new ExoS ADP-ribosyl transferase function to block host cell pyroptosis and maintain an intracellular niche. ExoS lacks overall amino acid homology to other bacterial ADP ribosyltransferases, and has a uniquely broad substrate specificity including small GTP-binding proteins and structural proteins (71). This multi substrate specificity is similar to that of multidrug transporters (72), and the hydrophobic reactions between ExoS and its ADP-ribosylated substrates has been previously compared to the interaction of a multidrug transporter and its ligand (23). We and other groups have shown ExoS still has unknown substrates (9, 10).

Here, we sought to identify new ExoS substrates using biochemical techniques, such as protein immunoprecipitation and mass spectrometry. During the characterization of the mono ADPr binding reagent, we were able to confirm the existence of unidentified ExoS substrates. In the initial ADPr binding reagent western blot, we observed bands outside the known range of ExoS substrates (Fig. 4). One third of the known ExoS substrates are around sixty-eight kDa, while most of the rest run around 23 kDa. We observed bands above and between these sizes, confirming the existence of unidentified ExoS substrates in corneal epithelial cells.

While the mono ADPr binding protein was suitable for western blotting and immunofluorescence, it was unsuitable for immunoprecipitation in our hands. This may be due to the mono ADPr binding reagent not appearing as previously described when run on total protein gels (Figs. 6 and 8), which may be the result of reagent degradation. Attempts at optimization were made, including using DSS to crosslink the mono ADPr binding reagent to magnetic protein A/G beads (Fig. 7). However, we were unable to pull down any ADP-ribosylated proteins.

While we were unable to identify new ExoS substrates through immunoprecipitating total corneal cell lysates, targeted immunoprecipitation may provide more success. As caspase-4 expression is required for ExoS ADP-ribosyltransferase-mediated delay of cell death, ExoS potentially ADP-ribosylates a protein in the caspase-4 inflammasome pathway. As an alternative strategy, we plan to express GFP-tagged noncanonical inflammasome components in mammalian cells. We can then immunoprecipitate for the GFP tag, and directly check for ADP-ribosylation.

In an attempt to identify uncategorized ExoS substrates without protein enrichment, mass spectrometry was conducted in collaboration with the Kirk lab and performed by Seby Edassery. In our preliminary round of mass spectrometry, we identified nine proteins with ADP-ribosyl modifications of arginine residues. Unfortunately, we identified no known ExoS substates, and not all post translational modifications were detected upon ExoS intoxication, suggesting only background signal was detected (Table 3). Intracellular T3SS was used to FACS sort corneal epithelial cells to enrich for internalized *P. aeruginosa* at the cellular level (Fig. 10). We then enriched cells for mass spectrometry through FACS sorting via an inducible intracellular T3SS construct (Table 4). This enrichment was not enough as again, we were unable to identify any

known ExoS substrates and the ADP ribosyl modification was found in samples lacking ExoS (Table 5). As an alternative method of enrichment, we plan to purify ExoS and perform invitro reaction of corneal epithelia cell lysate. Potential caveats for this experiment include unique ADP-ribosyl modifications in vitro than observed in corneal epithelial cells.

We also tested alternative methods of protein enrichment through immunoprecipitation. Previously, labeled NAD has been used to tag ExoS ADP-ribosylated substrates. While we were able to detect biotin-labeled NAD+, we found downsides with this approach. A dominant nonspecific band was observed in all treatments using biotin-labeled NAD+. We also observed a less robust banding pattern when infected with *P. aeruginosa* that expresses ExoS (Fig. 9). This is consistent with the idea of ExoS being unable to use modified NAD to ADP-ribosylate all substrates. Thus, this would not be an ideal approach to identify all ExoS substrates.

We then sought to detect new substrates through the creation of a BioId ExoS-BirA fusion protein. BirA, a promiscuous biotin ligase, when fused to ExoS would biotinylate any protein interacting with ExoS. Biotinylated proteins could then be captured via immunoprecipitation and identified via mass spectrometry. While we were able to create an ExoS-BirA fusion plasmid, we were unable to express the fusion protein (Fig.11). In the future, we plan to express the ExoS-BirA fusion protein directly in mammalian cells.

Because mass spectrometry on the cell lysates also shows total protein changes, we sought to analyze the data and identify how protein expression changes upon *P. aeruginosa* infection when compared to an uninfected control. We identified that protein expression, through translation and indicators of epigenetic modification, was upregulated upon infection (Figs. 12 and 13). General metabolic processes and some cell signaling pathways were downregulated upon infection. These findings suggest that upon infection corneal cells shift away from general

metabolism to upregulate protein expression, potentially to generate immune responses. We also identified many proteins upregulated upon *P. aeruginosa* infection were also upregulated during infection by other intracellular enteric pathogens, such as *Salmonella* and *Shigella*. Many of these proteins were also upregulated independently of ExoS, potentially illustrating the nature of *P. aeruginosa* as an intracellular pathogen. This finding could be clinically relevant, potentially allowing for targeted treatment options similar to other intracellular pathogens. We then compared the difference in protein expression during *P. aeruginosa* infection with or without ExoS. We identified a broad list of proteins uniquely regulated by infection with or without ExoS (Fig. 14). These findings further demonstrate host cell responses particular to *P. aeruginosa* infection modified by ExoS.

In the course of investigating new tools to detect ADP-ribosylation, we were also able to develop a method to visualize T3SS-targeted cells simultaneously with intracellular *P. aeruginosa* (Figs. 3 and 15). During immunofluorescence of the mono ADP-ribose binding reagent, we identified robust and textured fluorescence, suggesting that the signal is localized to cytoskeletal proteins. This is consistent with the literature, as ExoS ADP-ribosylates some structural and vesicle transport proteins (28, 31-33). By developing an ImageJ macro, we determined that the percentage of T3 intoxicated cells varies across cell type (Fig. 16 and Table 6). In HeLa cells, upwards of 90% cells are intoxicated via ExoS, which is vastly greater than the amount of intoxication seen in corneal epithelial cells. This higher intoxication is consistent with prior findings based on HeLa cell rounding as a way to measure ExoS delivery (70). Also contributing to the intoxication difference, *P. aeruginosa* preferentially invades the basolateral edge of polarized cells (69); access to the basolateral side is dependent on cell confluency. To determine the effect that intracellular *P. aeruginosa* has on T3 intoxication, we decided to treat

corneal epithelial cells with PI3 kinase inhibitors, which are known to block internalization. We found that when bacterial internalization is prevented, the delivery of T3SS effectors into corneal epithelial cells vastly diminishes (Fig. 17). In the future, we plan to use this method to determine the importance of internalization in vivo, and of cytotoxic strains of *P. aeruginosa.*

Together, our aims and findings support the importance of *P. aeruginosa* taking on an intracellular lifestyle. We show evidence of unidentified ExoS substrates that interfere with host cell pyroptosis in response to intracellular bacteria. We also show the necessity of *P. aeruginosa* internalization prior to T3 intoxication. As the intracellular nature of *P. aeruginosa* remains understudied, more research is needed to understand how *P. aeruginosa* infects the cornea and other epithelial sites.

REFERNCE LIST

1. Nathwani D, Raman G, Sulham K, Gavaghan M, Menon V. 2014. Clinical and economic consequences of hospital-acquired resistant and multidrug-resistant Pseudomonas aeruginosa infections: a systematic review and meta-analysis. Antimicrobial Resistance and Infection Control 3:32.

2. Green M, Apel A, Stapleton F. 2008. Risk factors and causative organisms in microbial keratitis. Cornea 27:22-7.

3. Schaefer F. 2001. Bacterial keratitis: a prospective clinical and microbiological study. British Journal of Ophthalmology 85:842-847.

4. Fleiszig SMJ, Kroken AR, Nieto V, Grosser MR, Wan SJ, Metruccio MME, Evans DJ. 2020. Contact lens-related corneal infection: Intrinsic resistance and its compromise. Prog Retin Eye Res 76:100804.

5. Comolli JC, Hauser AR, Waite L, Whitchurch CB, Mattick JS, Engel JN. 1999. Pseudomonas aeruginosa gene products PilT and PilU are required for cytotoxicity in vitro and virulence in a mouse model of acute pneumonia. Infect Immun 67:3625-30.

6. Kroken AR, Chen CK, Evans DJ, Yahr TL, Fleiszig SMJ. 2018. The Impact of ExoS on Pseudomonas aeruginosa Internalization by Epithelial Cells Is Independent of fleQ and Correlates with Bistability of Type Three Secretion System Gene Expression. mBio 9.

7. Kroken AR, Gajenthra Kumar N, Yahr TL, Smith BE, Nieto V, Horneman H, Evans DJ, Fleiszig SMJ. 2022. Exotoxin S secreted by internalized Pseudomonas aeruginosa delays lytic host cell death. PLoS Pathog 18:e1010306.

8. Kroken AR.

9. Riese MJ, Goehring UM, Ehrmantraut ME, Moss J, Barbieri JT, Aktories K, Schmidt G. 2002. Auto-ADP-ribosylation of Pseudomonas aeruginosa ExoS. J Biol Chem 277:12082-8.

10. Coburn J, Dillon ST, Iglewski BH, Gill DM. 1989. Exoenzyme S of Pseudomonas aeruginosa ADP-ribosylates the intermediate filament protein vimentin. Infect Immun 57:996-8.

11. Blocker A, Jouihri N, Larquet E, Gounon P, Ebel F, Parsot C, Sansonetti P, Allaoui A. 2001. Structure and composition of the Shigella flexneri "needle complex", a part of its type III secreton. Mol Microbiol 39:652-63.

12. Galle M, Carpentier I, Beyaert R. 2012. Structure and function of the Type III secretion system of Pseudomonas aeruginosa. Curr Protein Pept Sci 13:831-42.

13. Fleiszig SM, Wiener-Kronish JP, Miyazaki H, Vallas V, Mostov KE, Kanada D, Sawa T, Yen TS, Frank DW. 1997. Pseudomonas aeruginosa-mediated cytotoxicity and invasion correlate with distinct genotypes at the loci encoding exoenzyme S. Infect Immun 65:579-86.

14. Finck-Barbancon V, Goranson J, Zhu L, Sawa T, Wiener-Kronish JP, Fleiszig SM, Wu C, Mende-Mueller L, Frank DW. 1997. ExoU expression by Pseudomonas aeruginosa correlates with acute cytotoxicity and epithelial injury. Mol Microbiol 25:547-57.

15. Sato H, Frank DW. 2004. ExoU is a potent intracellular phospholipase. Molecular Microbiology 53:1279-1290.

16. Hritonenko V, Mun JJ, Tam C, Simon NC, Barbieri JT, Evans DJ, Fleiszig SM. 2011. Adenylate cyclase activity of Pseudomonas aeruginosa ExoY can mediate bleb-niche formation in epithelial cells and contributes to virulence. Microb Pathog 51:305-12.

17. Ochoa CD, Alexeyev M, Pastukh V, Balczon R, Stevens T. 2012. Pseudomonas aeruginosa Exotoxin Y Is a Promiscuous Cyclase That Increases Endothelial Tau Phosphorylation and Permeability. Journal of Biological Chemistry 287:25407-25418.

18. Silistre H, Raoux-Barbot D, Mancinelli F, Sangouard F, Dupin A, Belyy A, Deruelle V, Renault L, Ladant D, Touqui L, Mechold U. 2021. Prevalence of ExoY Activity in Pseudomonas aeruginosa Reference Panel Strains and Impact on Cytotoxicity in Epithelial Cells. Front Microbiol 12:666097.

19. Iglewski BH, Sadoff J, Bjorn MJ, Maxwell ES. 1978. Pseudomonas aeruginosa exoenzyme S: an adenosine diphosphate ribosyltransferase distinct from toxin A. Proc Natl Acad Sci U S A 75:3211-5.

20. Yahr TL, Barbieri JT, Frank DW. 1996. Genetic relationship between the 53- and 49-kilodalton forms of exoenzyme S from Pseudomonas aeruginosa. J Bacteriol 178:1412-9.

21. Frithz-Lindsten E, Du Y, Rosqvist R, Forsberg A. 1997. Intracellular targeting of exoenzyme S of Pseudomonas aeruginosa via type III-dependent translocation induces phagocytosis resistance, cytotoxicity and disruption of actin microfilaments. Mol Microbiol 25:1125-39.

22. Pederson KJ, Vallis AJ, Aktories K, Frank DW, Barbieri JT. 1999. The amino-terminal domain of Pseudomonas aeruginosa ExoS disrupts actin filaments via small-molecular-weight GTP-binding proteins. Mol Microbiol 32:393-401.

23. Barbieri JT, Sun J. 2004. Pseudomonas aeruginosa ExoS and ExoT. Rev Physiol Biochem Pharmacol 152:79-92.

24. Goehring UM, Schmidt G, Pederson KJ, Aktories K, Barbieri JT. 1999. The N-terminal domain of Pseudomonas aeruginosa exoenzyme S is a GTPase-activating protein for Rho GTPases. J Biol Chem 274:36369-72.

25. Garrity-Ryan L, Kazmierczak B, Kowal R, Comolli J, Hauser A, Engel JN. 2000. The arginine finger domain of ExoT contributes to actin cytoskeleton disruption and inhibition of internalization of Pseudomonas aeruginosa by epithelial cells and macrophages. Infect Immun 68:7100-13.

26. Cowell BA, Chen DY, Frank DW, Vallis AJ, Fleiszig SM. 2000. ExoT of cytotoxic Pseudomonas aeruginosa prevents uptake by corneal epithelial cells. Infect Immun 68:403-6.

27. Ganesan AK, Frank DW, Misra RP, Schmidt G, Barbieri JT. 1998. Pseudomonas aeruginosa exoenzyme S ADP-ribosylates Ras at multiple sites. J Biol Chem 273:7332-7.

28. Barbieri AM, Sha Q, Bette-Bobillo P, Stahl PD, Vidal M. 2001. ADP-ribosylation of Rab5 by ExoS of Pseudomonas aeruginosa affects endocytosis. Infect Immun 69:5329-34.

29. Riese MJ, Wittinghofer A, Barbieri JT. 2001. ADP ribosylation of Arg41 of Rap by ExoS inhibits the ability of Rap to interact with its guanine nucleotide exchange factor, C3G. Biochemistry 40:3289-94.

30. Simon NC, Barbieri JT. 2014. Exoenzyme S ADP-ribosylates Rab5 effector sites to uncouple intracellular trafficking. Infect Immun 82:21-8.

31. Rocha CL, Rucks EA, Vincent DM, Olson JC. 2005. Examination of the coordinate effects of Pseudomonas aeruginosa ExoS on Rac1. Infect Immun 73:5458-67.

32. Fraylick JE, Rucks EA, Greene DM, Vincent TS, Olson JC. 2002. Eukaryotic cell determination of ExoS ADP-ribosyltransferase substrate specificity. Biochem Biophys Res Commun 291:91-100.

33. Maresso AW, Baldwin MR, Barbieri JT. 2004. Ezrin/radixin/moesin proteins are high affinity targets for ADP-ribosylation by Pseudomonas aeruginosa ExoS. J Biol Chem 279:38402-8.

34. Maresso AW, Deng Q, Pereckas MS, Wakim BT, Barbieri JT. 2007. Pseudomonas aeruginosa ExoS ADP-ribosyltransferase inhibits ERM phosphorylation. Cellular Microbiology 9:97-105.

35. DiNovo AA, Schey KL, Vachon WS, McGuffie EM, Olson JC, Vincent TS. 2006. ADP-ribosylation of cyclophilin A by Pseudomonas aeruginosa exoenzyme S. Biochemistry 45:4664-73.

36. Feltman H, Schulert G, Khan S, Jain M, Peterson L, Hauser AR. 2001. Prevalence of type III secretion genes in clinical and environmental isolates of Pseudomonas aeruginosa. Microbiology 147:2659-2669.

37. Fleiszig SM, Zaidi TS, Preston MJ, Grout M, Evans DJ, Pier GB. 1996. Relationship between cytotoxicity and corneal epithelial cell invasion by clinical isolates of Pseudomonas aeruginosa. Infect Immun 64:2288-94.

38. Kumar NG, Nieto V, Kroken AR, Jedel E, Grosser MR, Hallsten ME, Mettrucio MME, Yahr TL, Evans DJ, Fleiszig SMJ. 2022. Pseudomonas aeruginosa Can Diversify after Host Cell Invasion to Establish Multiple Intracellular Niches. mBio 13:e0274222.

39. Chi E, Mehl T, Nunn D, Lory S. 1991. Interaction of Pseudomonas aeruginosa with A549 pneumocyte cells. Infect Immun 59:822-8.

40. Fleiszig SM, Zaidi TS, Fletcher EL, Preston MJ, Pier GB. 1994. Pseudomonas aeruginosa invades corneal epithelial cells during experimental infection. Infect Immun 62:3485-93.

41. Fleiszig SM, Zaidi TS, Pier GB. 1995. Pseudomonas aeruginosa invasion of and multiplication within corneal epithelial cells in vitro. Infect Immun 63:4072-7.

42. Kierbel A, Gassama-Diagne A, Mostov K, Engel JN. 2005. The Phosphoinositol-3-Kinase–Protein Kinase B/Akt Pathway Is Critical for Pseudomonas aeruginosa Strain PAK Internalization. Molecular Biology of the Cell 16:2577-2585.

43. Kierbel A, Gassama-Diagne A, Rocha C, Radoshevich L, Olson J, Mostov K, Engel J. 2007. Pseudomonas aeruginosa exploits a PIP3-dependent pathway to transform apical into basolateral membrane. Journal of Cell Biology 177:21-27.

44. Angus AA, Evans DJ, Barbieri JT, Fleiszig SM. 2010. The ADP-ribosylation domain of Pseudomonas aeruginosa ExoS is required for membrane bleb niche formation and bacterial survival within epithelial cells. Infect Immun 78:4500-10.

45. Ince D, Sutterwala FS, Yahr TL. 2015. Secretion of Flagellar Proteins by the Pseudomonas aeruginosa Type III Secretion-Injectisome System. Journal of Bacteriology 197:2003-2011.

46. Kanneganti TD, Lamkanfi M, Nunez G. 2007. Intracellular NOD-like receptors in host defense and disease. Immunity 27:549-59.

47. Martinon F, Burns K, Tschopp J. 2002. The inflammasome: a molecular platform triggering activation of inflammatory caspases and processing of proIL-beta. Mol Cell 10:417-26.

48. Elliott JM, Rouge L, Wiesmann C, Scheer JM. 2009. Crystal structure of procaspase-1 zymogen domain reveals insight into inflammatory caspase autoactivation. J Biol Chem 284:6546-53.

49. Poltorak A, He X, Smirnova I, Liu MY, Van Huffel C, Du X, Birdwell D, Alejos E, Silva M, Galanos C, Freudenberg M, Ricciardi-Castagnoli P, Layton B, Beutler B. 1998. Defective LPS signaling in C3H/HeJ and C57BL/10ScCr mice: mutations in Tlr4 gene. Science 282:2085-8.

50. Hagar JA, Powell DA, Aachoui Y, Ernst RK, Miao EA. 2013. Cytoplasmic LPS activates caspase-11: implications in TLR4-independent endotoxic shock. Science 341:1250-3.

51. Shi J, Zhao Y, Wang Y, Gao W, Ding J, Li P, Hu L, Shao F. 2014. Inflammatory caspases are innate immune receptors for intracellular LPS. Nature 514:187-192.

52. Wandel MP, Kim B-H, Park E-S, Boyle KB, Nayak K, Lagrange B, Herod A, Henry T, Zilbauer M, Rohde J, Macmicking JD, Randow F. 2020. Guanylate-binding proteins convert cytosolic bacteria into caspase-4 signaling platforms. Nature Immunology 21:880-891.

53. Santos JC, Boucher D, Schneider LK, Demarco B, Dilucca M, Shkarina K, Heilig R, Chen KW, Lim RYH, Broz P. 2020. Human GBP1 binds LPS to initiate assembly of a caspase-4 activating platform on cytosolic bacteria. Nature Communications 11.

54. Aglietti RA, Estevez A, Gupta A, Ramirez MG, Liu PS, Kayagaki N, Ciferri C, Dixit VM, Dueber EC. 2016. GsdmD p30 elicited by caspase-11 during pyroptosis forms pores in membranes. Proceedings of the National Academy of Sciences 113:7858-7863.

55. Liu Z, Wang C, Yang J, Chen Y, Zhou B, Abbott DW, Xiao TS. 2020. Caspase-1 Engages Full-Length Gasdermin D through Two Distinct Interfaces That Mediate Caspase Recruitment and Substrate Cleavage. Immunity 53:106-114 e5.

56. Cisz M, Lee PC, Rietsch A. 2008. ExoS controls the cell contact-mediated switch to effector secretion in Pseudomonas aeruginosa. J Bacteriol 190:2726-38.

57. Urbanowski ML, Brutinel ED, Yahr TL. 2007. Translocation of ExsE into Chinese hamster ovary cells is required for transcriptional induction of the Pseudomonas aeruginosa type III secretion system. Infect Immun 75:4432-9.

58. Robertson DM, Li L, Fisher S, Pearce VP, Shay JW, Wright WE, Cavanagh HD, Jester JV. 2005. Characterization of growth and differentiation in a telomerase-immortalized human corneal epithelial cell line. Invest Ophthalmol Vis Sci 46:470-8.

59. Huang da W, Sherman BT, Lempicki RA. 2009. Bioinformatics enrichment tools: paths toward the comprehensive functional analysis of large gene lists. Nucleic Acids Res 37:1-13.

60. Huang da W, Sherman BT, Lempicki RA. 2009. Systematic and integrative analysis of large gene lists using DAVID bioinformatics resources. Nat Protoc 4:44-57.

61. Gibson BA, Conrad LB, Huang D, Kraus WL. 2017. Generation and Characterization of Recombinant Antibody-like ADP-Ribose Binding Proteins. Biochemistry 56:6305-6316.

62. Roux KJ, Kim DI, Burke B, May DG. 2018. BioID: A Screen for Protein-Protein Interactions. Current Protocols in Protein Science 91.

63. Aiello D, Williams JD, Majgier-Baranowska H, Patel I, Peet NP, Huang J, Lory S, Bowlin TL, Moir DT. 2010. Discovery and characterization of inhibitors of Pseudomonas aeruginosa type III secretion. Antimicrob Agents Chemother 54:1988-99.

64. Verove J, Bernarde C, Bohn Y-ST, Boulay F, Rabiet M-J, Attree I, Cretin F. 2012. Injection of Pseudomonas aeruginosa Exo Toxins into Host Cells Can Be Modulated by Host Factors at the Level of Translocon Assembly and/or Activity. PLoS ONE 7:e30488.

65. Goldberg MB. 2001. Actin-based motility of intracellular microbial pathogens. Microbiol Mol Biol Rev 65:595-626, table of contents.

66. Nieto V, Kroken AR, Grosser MR, Smith BE, Metruccio MME, Hagan P, Hallsten ME, Evans DJ, Fleiszig SMJ. 2019. Type IV Pili Can Mediate Bacterial Motility within Epithelial Cells. mBio 10.

67. Tegtmeyer N, Soltan Esmaeili D, Sharafutdinov I, Knorr J, Naumann M, Alter T, Backert S. 2022. Importance of cortactin for efficient epithelial NF-κB activation by Helicobacter pylori, Salmonella enterica and Pseudomonas aeruginosa, but not Campylobacter spp. European Journal of Microbiology and Immunology 11:95-103.

68. BougnèRes L, Girardin SPE, Weed SA, Karginov AV, Olivo-Marin J-C, Parsons JT, Sansonetti PJ, Van Nhieu GT. 2004. Cortactin and Crk cooperate to trigger actin polymerization during Shigella invasion of epithelial cells. Journal of Cell Biology 166:225-235.

69. Fleiszig SM, Evans DJ, Do N, Vallas V, Shin S, Mostov KE. 1997. Epithelial cell polarity affects susceptibility to Pseudomonas aeruginosa invasion and cytotoxicity. Infect Immun 65:2861-7.

70. Sun J, Barbieri JT. 2004. ExoS Rho GTPase-activating Protein Activity Stimulates Reorganization of the Actin Cytoskeleton through Rho GTPase Guanine Nucleotide Disassociation Inhibitor. Journal of Biological Chemistry 279:42936-42944.

71. Krueger KM, Barbieri JT. 1995. The family of bacterial ADP-ribosylating exotoxins. Clinical Microbiology Reviews 8:34-47.

72. Marchalonis JJ, Schluter SF, Bernstein RM, Hohman VS. 1998. Antibodies of sharks: revolution and evolution. Immunol Rev 166:103-22.

VITA

The author, Adam Thota, was born in Muskego, WI on March 31, 1998 to Dr. Raj and Cindy Thota. He attended Wisconsin Lutheran College where he earned a Bachelor of Science in Biology in May of 2021. After graduation, Adam matriculated into the Loyola University Chicago Stritch School of Medicine master's degree (MS) program and began his graduate education in the Biochemistry and Molecular Biology (BMB) program under the mentorship of Dr. Abby Kroken.

After completion of his graduate studies, Adam will continue to work under the supervision of Dr. Abby Kroken while pursuing a PhD at Loyola University Chicago.